Underground hydrogen storage in salt caverns: the potential of bedded salt formations

Romay Saville
(6201024)

MSc Thesis Energy Science
February 2024

Utrecht University supervisor: Dr. Ir. Hamed Aslannejad
Antea Group supervisor: Søren Winkel

Course code: GEO4-2510
Faculty of Geosciences

Word count: 12.519

Utrecht University

Summary

Large-scale energy storage solutions are essential to address the intermittent nature of renewable energy sources. Hydrogen is found to be a promising option for energy storage due to its renewable nature. When integrating energy storage systems into the electricity grid, the storage systems need to have a capacity in the MW range, these are considered large-scale storage systems. Hydrogen can provide this storage capacity due to its high energy density, compared to other energy storage mechanisms.

Underground hydrogen storage (UHS) has minimal social and environmental impacts compared to large-scale surface energy storage. UHS in salt caverns is mostly discussed in domal salt formations, however the use of bedded salt formations is gaining interest as these formations are more commonly present in certain countries, such as the Netherlands. To this date the only UHS caverns in bedded salt formations are three smaller caverns in Teesside in the United Kingdom. The hydrogen storage potential in other bedded salt formations has not been fully analysed. The Netherlands has an increased need for energy storage due to the various renewable developments in the North Sea. With these projects the Netherlands will play a key role in the transport of the generated energy to other countries, potentially using hydrogen as an energy carrier.

To analyse the storage potential in bedded salt formations, a comprehensive methodology has been employed. Firstly, the technical requirements for a salt cavern storing hydrogen were defined. Secondly, a model is developed to analyse the cyclic injection and extraction (IE) processes of hydrogen in salt caverns, investigating IE rates under various well configurations and IE velocities. It then finds the storage capacity of the cavern based on the working gas volume, and plots the loading profile of each cavern. The final section of the research creates an interactive map which displays the storage capacity of a single cavern in various locations in the Netherlands, which have been chosen in this research based on the presence of bedded salts in the area.

The main cavern requirements are based on the salt formation depth and thickness. The pressure range is found to be 30-80% of the overburden pressure. The injection and extraction rates are only found to reach the maximum rate of 1 MPa/day when using a second well. The modelled cavern was found to have a storage capacity of 14.66 GWh. According to a residual load profile the potential for variable loading was analysed, and the modelled cavern was found to be too small to match the residual load of the Netherlands in 2030.

In conclusion, bedded salt formations offer significant potential for UHS. The Netherlands contains many suitable locations for UHS in bedded salt formations, with the size of the caverns differing significantly throughout the country. The suitable salt formations are located mostly in the East and North of the Netherlands. Further research is required to explore the integration of specific caverns into local or national energy systems, and the costs associated with this storage technique.

Contents

Nomenclature

$\dot{E}$	Energetic flow rate
$\dot{m}$	Mass flow
$\dot{V}$	Volume flow
ρ	Density
D	Depth
d	Diameter
h	Height
n	Moles of gas
P	Pressure
Q	Flow rate
R	Universal gas constant
r	Ratio
T	Temperature
V	Volume
v	Velocity
v_{sp}	Specific volume
ESS	Energy Storage system
IE	Injection and extraction
LHV	Lower heating value
SWV	Single-well-vertical
TRL	Technology readiness level
UGS	Underground gas storage
UHS	Underground hydrogen storage

List of Tables

List of Figures

1 Introduction

1.1 Scientific and societal relevance

In order to mitigate climate change and to bring emissions to net zero in 2050, the United Nations signed the Paris Agreement in 2015 (UNFCCC, 2015). Within Europe, the European Council have created the Fit for 55 package, a comprehensive framework deigned to assist member states to reduce their greenhouse gas emissions by 55% in 2030 compared to values recorded in 1990. A key component of this framework is the increase in use and the integration of renewable energy sources into the current energy system (European Council, n.d.).

When incorporating renewable energy sources in the current energy mix, a few main challenges arise. The first of which being the intermittency of the renewables due to their production being reliant on certain weather conditions. This intermittency can introduce a volatility in the electricity prices. Additionally renewable sources lack a dispatchability, as opposed to electricity generation by using coal-, natural gas- or oil-fired power plants (Matos et al., 2019). To address and mitigate the effects of these challenges, energy storage systems (ESS) must be incorporated into the electricity grid. ESS serve as mechanisms to store energy when the demand is low, and dispatch energy into the grid when the demand is high (Rahman et al., 2020).

ESS can be divided into five main categories: chemical, electrochemical, electrical, mechanical and thermal storage. The type of storage method chosen depends on the volumes of energy that must be stored. For small-scale storage (< 10 MW), electrochemical, electrical and thermal storage are the most used systems. For large-scale storage, mechanical and chemical storage are deployed (Matos et al., 2019; Rahman et al., 2020). To be able to incorporate ESS into the electricity grid, the storage mechanisms must have a capacity which is large enough to meet the demand of the power grid or region. Only large-scale storage systems have this capacity. The incorporation of large-scale ESS provides the ability to balance the supply and demand of the grid, ensure energy security and to better manage the energy grid. Mechanical storage, such as pumped hydro and compressed air energy storage, can provide the storage capacity required, however their low storage density is a major drawback. The advantage of chemical storage systems, such as hydrogen, is that they provide a significantly higher energy density with the same storage capacity. Hydrogen is seen as a promising energy storage carrier due to its renewable nature. Energy storage using hydrogen consists of a Power-to-Gas principle, which entails that hydrogen

is formed using electricity, in the case of green hydrogen this is renewable electricity (Caglayan et al., 2020).

1.2 Underground hydrogen storage

Hydrogen can either be stored above ground, in surface tanks, or underground (Figure 1). Underground hydrogen storage (UHS) has been a recent topic of interest as the social and environmental impacts are minimized compared to larger-scale surface storage. There are several advantages to UHS, one of which being security as the storage systems are less susceptible to fires, floods or human attacks. Furthermore, UHS locations are generally larger than surface storage tanks. The building of a UHS is also economically favorable, when compared to a surface storage facility with a similar capacity. To illustrate this an example is taken in crude oil storage, in which surface storage is $\$15 - 18$ per barrel and underground storage is around \$3 per barrel (Matos et al., 2019; Peng et al., 2023). There are currently four major options for UHS, displayed in Figure 1 along with their typical storage capacities.

The first UHS mechanism being lined rock caverns, which are man-made rock caverns covered with a layer of concrete and then lined with steel or plastic. Their man-made nature causes the caverns to have no risk of impurities. The use of steel as a liner is under debate due to the embrittlement of steel when exposed to hydrogen over a longer period of time (Hematpur et al., 2023; Hydrogen TCP-Task 42, 2023).

Depleted hydrocarbon reservoirs are currently the most common storage sites for natural gas. These reservoirs are located in porous, permeable sedimentary rock formations, above which lies an impermeable caprock. Hydrocarbon reservoirs have proven to store natural gas for millions of years, suggesting that these would also be suitable for hydrogen storage. However, hydrogen chemically differs from natural gas as it is more reactive, introducing the possibility of reactions with surrounding minerals, water, or microbiomes (Hematpur et al., 2023; Hydrogen TCP-Task 42, 2023).

Aquifers are also a common underground gas storage (UGS) system, having the same porous permeable characteristics and being covered by an impermeable caprock. A geological survey however is needed to prove the integrity of the caprock, which requires more resources (Hematpur et al., 2023; Hydrogen TCP-Task 42, 2023).

Salt caverns are man-made caverns in rock salt layers. These are created through salt solution mining; the controlled injection of fresh water into the deposits, dissolving the rock salt and forming a cavern. The geomechan-

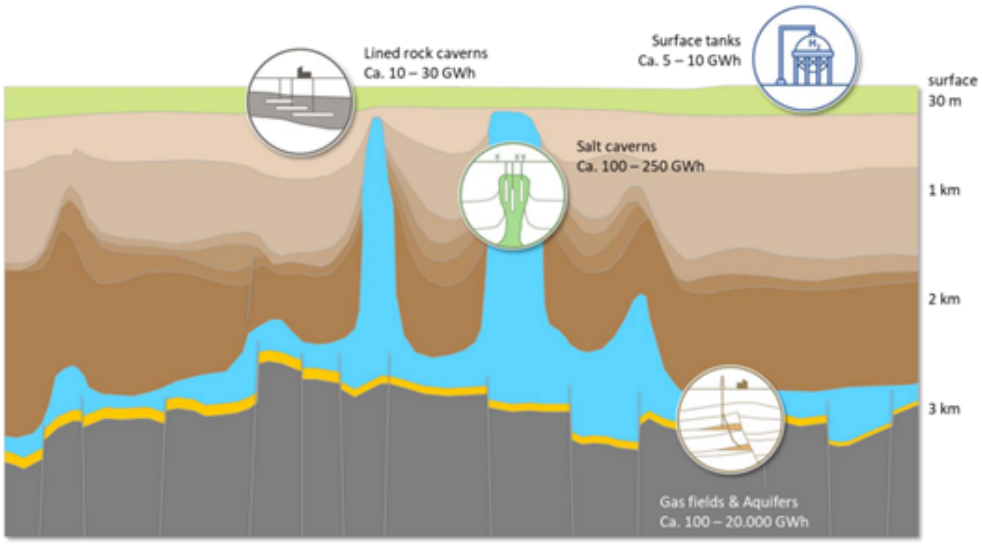

Figure 1. *An overview of the technologies considered for hydrogen storage, including their general depth and typical ranges of storage capacities (Hydrogen TCP-Task 42, 2023).*

ical properties of salt make it an exceptional medium for gas storage. One being is its viscoplastic behavior at different temperatures and pressures. This property protects the cavern from the formation and spread of faults and ensures the relaying tightness in the cavern, which is essential for gas storage. The cavern also has a low porosity and permeability, which prevents leakage of gas. Furthermore, rock salt is chemically inert towards hydrogen, limiting the possibility of reactions (Hematpur et al., 2023; Hydrogen TCP-Task 42, 2023; Małachowska et al., 2022; Zhang et al., 2021).

To date, UHS has only been implemented using salt caverns. Three smaller caverns in Teeside, United Kingdom (UK), are used as a buffer in a shared (petro)chemical network. These caverns are located in a bedded salt formation at a depth of 365m and are operated at a pressure of 45 bar. In Texas, United States of America (USA), three much larger caverns act as reserves to cover operational shutdowns in the nearby (petro)chemical industry. These caverns are situated in salt diapers at 1000-1340m depth and operated at pressures ranging from 55-202 bar. The three caverns fill into a hydrogen pipeline, which runs for hundreds of kilometers (Crotogino, 2022; Groenenberg et al., 2020; Matos et al., 2019). As there are working projects of UHS in salt caverns, the technology places at a Technology Readiness Level (TRL) of 9. This placement is however only for long-term and low-cyclic storage applications. Fast-cyclic applications are needed to balance the electricity grid, as there are no such caverns currently, the technology is placed at a TRL of 5-6 (Hydrogen TCP-Task 42, 2023).

1.3 Previous Research

Hydrogen and UHS have gained interest as hydrogen is one of the few options for the storage of large quantities of energy, which can be used to balance out the intermittency of renewable energy sources. UHS is of importance as it is one of the only storage options which can accommodate the large storage capacities required (Crotogino et al., 2010). Rahman et al., 2020 gave a review of energy storage technologies, showing the possibilities and calculating the costs associated with each technology. UHS was identified as a suitable option for bulk energy storage and shown to lower the electricity cost by 6-18% when compared to surface storage (Rahman et al., 2020; Steward et al., 2009). Around the same time an overview of large-scale underground ESS was published, in which salt caverns were found to be the best option for storing hydrogen as salt is gas tight and inert with respect to hydrogen. A list of certain cavern requirements, with regard to hydrogen storage, is given in the publication (Matos et al., 2019). The technical aspects and cavern design are further outlined and modelled in Abreu et al., 2023, which also outlines a cavern sizing protocol and the effects of salt creep on the cavern lifetime.

Papadias and Ahluwalia, 2021 analysed certain technical and economical properties of bulk hydrogen storage in pipes, lined rock caverns and salt caverns, and compared these. This was done partly through calculating the lifetime costs of these three technologies and the effect of scaling up the storage capacity on the costs. It was then concluded that UHS in salt caverns is the most economically favorable technology when considering bulk storage, as salt caverns are much larger and require less caverns to scale up storage. UHS in bedded salts differs to that in salt domes or diapers, due to the difference in thickness and rock salt composition. The influence of the interlayer content in the rock salt formation on the stability of the cavern over time, was evaluated by Zhang et al., 2021. It was found that caverns in bedded salts with higher interlayer contents are more stable than those with no to low interlayer content. The increased interlayer content also decreased the volume shrinkage in UGS caverns. Other research into storage in bedded salts showed that a two-well-horizontal cavern design was best suited to thinly bedded salt formations (Peng et al., 2023). Schwab et al., 2022, present a guideline for characterizing the present microbiomes in salt caverns and thus also gaining insight into the potential effects on the hydrogen quality.

1.4 Storage potential in the Netherlands

The identification of suitable energy storage locations in the Netherlands has been of increased importance in the past few years. With this importance heavily being influenced by the need for an increase in energy security after the cut-off of Russian gas during the war in Ukraine, which forced the Netherlands to rely on other natural gas suppliers (Prisecaru, 2022). With the increasing renewable developments in the North Sea, the Netherlands will start to play an important role in the transport of energy to other countries in Europe, using hydrogen as an energy carrier (Brunner et al., 2022; Gasunie, n.d.). The Dutch Ministry of Economic Affairs and Climate made their hydrogen strategy public, stating that hydrogen transport and storage strategies will be researched and implemented (Ministry of Economic Affairs and Climate, 2020). To distribute this renewable energy, electrolyzers will be placed in major harbors, connected through a hydrogen network. This network will be installed by Gasunie, who aim to make the Netherlands the hydrogen port of Europe, by connecting this backbone internationally (Gasunie, n.d.).

To quantify the transition needs until 2050, TNO and EBN have developed several pathways for the energy system. Underground energy storage has been included in these pathways, along with the required storage potential for each pathway. The pathways suggest the need for UGS and UHS, both in the pathways up to 2030 and those between 2030-2050. The UHS will be in the form of salt caverns and depleted gas fields, with the majority of the storage capacity being in salt caverns, as the storage of hydrogen in gas fields has not yet been proven (van Gessel et al., 2021). The Netherlands contains several salt deposits, located in the North and the East of the country (Figure 2). The North of the Netherlands containing mainly salt structures such as salt domes, pillows and other formations. While the deposits in the East are classified as bedded salt deposits (Caglayan et al., 2020). Bedded salt deposits are wide, thin, and horizontal salt layers, alternating with non-salt interlayers (Zhang et al., 2021).

Currently, the salt domes in the North of the Netherlands are the location of a hydrogen storage pilot project by HyStock. This project consists of several salt caverns which will be used for the storage of natural gas and hydrogen, and then connected to the hydrogen network (HyStock, n.d.). The bedded salt formations in Twente contain hundreds of salt caverns, created for salt mining by Nobian, and located near larger cities. Several locations within this formation have also been identified as suitable locations for underground storage of gas, oil or (radioactive)waste (Altenburg, 2022; Groenenberg et al., 2020). There have been several projects in which the potential

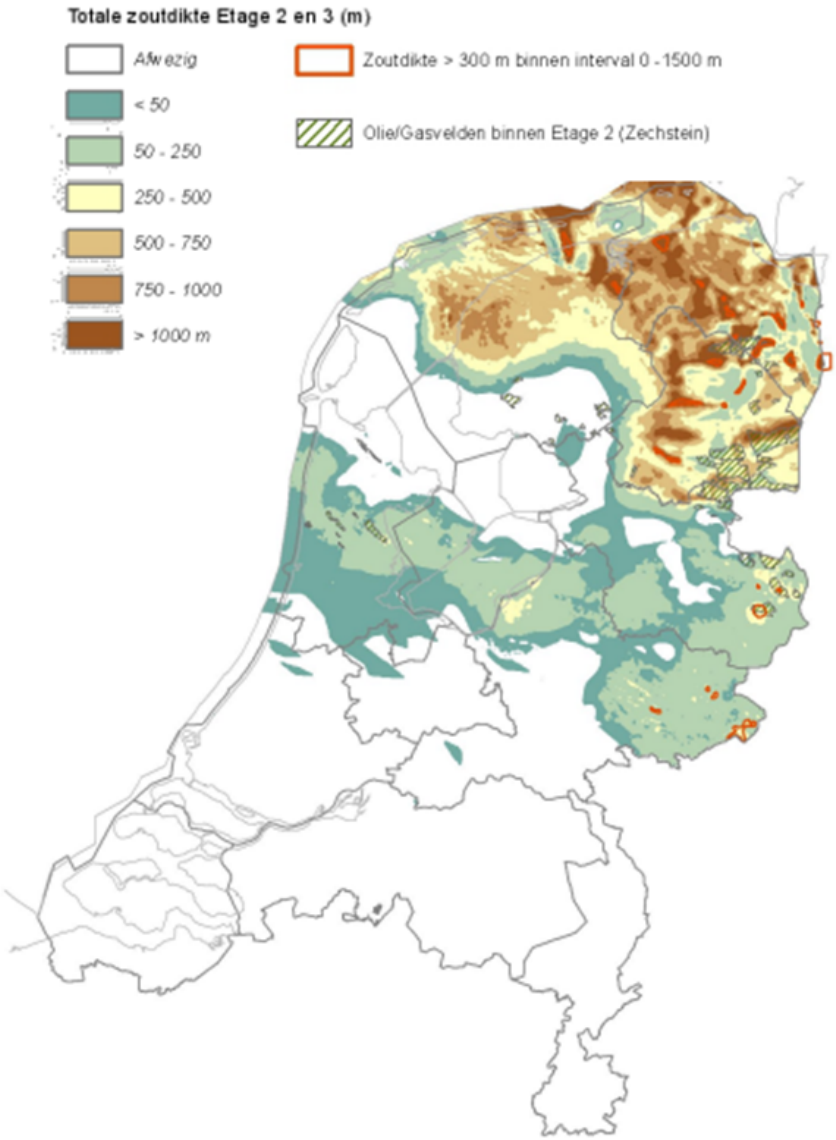

Figure 2. *Map showing the total thickness of salt layers within the Triassic and Zechstein formations. The red outlined areas have a salt layer of >300m thickness, within an interval of 0-1500m. The striped areas contain oil/gas fields, which are formed within the Zechstein group. (TNO, n.d.)*

of UHS in the Netherlands has been calculated. These calculations largely focused on the storage potential of salt domes in the North of the Netherlands (Juez-Larré et al., 2019, 2023). However, the storage potential of the bedded salt formations in the Netherlands has not yet been fully evaluated.

1.5 Research aim and questions

The aim of this research is to analyse the hydrogen storage potential of salt caverns in bedded salt formations. This potential will be analysed in three main processes. Firstly, literature research will be performed to identify the cavern requirements for UHS, also based on actual storage locations. This data will later be used to identify suitable bedded salt formations in the Netherlands. Secondly, a model will be created to model the injection and extraction of hydrogen into the cavern. The model will also provide insight into certain storage properties, including the IE rate and the storage capacity of each cavern. This will then be translated to the bedded salt formations in the Netherlands and used to identify potential storage sites. This research aim can be formulated in the following research question and sub questions.

What is the underground hydrogen storage potential of salt caverns in bedded salt formations?

1. What are the cavern requirements for hydrogen storage in salt caverns located in bedded salt formations?

2. What are the injection and extraction rates of the salt cavern?

3. What is the storage capacity based on the working volume of the salt cavern?

4. What is the potential storage capacity of a salt cavern in bedded salt formations in the Netherlands?

2 Geological background

This section will elaborate on the theoretical background with regards to the geology of bedded salt formations and the design of UHS caverns in these formations.

2.1 UHS in salt caverns

One of the key elements in UHS is understanding the geological composition of the salt formation. Salt mining has historically been an important industry in the Netherlands, which brings the advantage of detailed geological research and mapping of the present salt formations, as seen in Figure 2. The largest total thickness is seen in the North of the Netherlands, with some areas of medium thickness in the East. The map shows the total thickness of salt, and as some formations will be bedded salts, this thickness may be spread over a larger depth, which might not be compatible for UHS salt caverns. As noted in the introduction, the Netherlands mostly contains bedded salt deposits, which this research will focus on. These deposits are found within the Röt and Zechstein formations (NLOG, n.d.).

The salt deposits discussed when considering UHS are mostly composed of halite, which is a pure form of NaCl. This material has mineral properties which are advantageous for hydrogen storage, as discussed in previous sections. Salt formations are classified as an evaporite deposit, which have formed from a mineral-rich and semi-isolated water basin (Wijermans, 2013). Through evaporation of water the mineral content in the water increases. Each of these minerals have a certain solubility limit, which will lead to deposition once it is surpassed. This cycle of evaporation and deposition continues over time, eventually depositing a layer of salt of potentially varying composition. After deposition of the salt layers, the area may be covered by other rock formations, and potentially undergo compression, extension or other deformation mechanisms. The stress and pressure from deformation will effect the occurrence of halokinesis, the fluid-like movement of salt layers, which changes the shape and dimension of various salt deposits, forming salt pillows or domes. Bedded salt formations are the only formation in which halokinesis has not taken place (Wijermans, 2013).

2.2 Potential of bedded salt formations

When designing salt caverns for UHS, salt domes are often considered first. This mainly due to their sheer size and depth, which results in a large

storage area. However, bedded salt formations also show potential for storage and are already implemented in the UK. These formations are often used for salt mining, however the caverns formed for this industry do not always meet requirements to store hydrogen. Therefore a different cavern design might be required (Peng et al., 2023; Williams et al., 2022). There have been several studies on the energy storage potential of the bedded salt formations in the UK, with Williams et al., 2022 assessing the hydrogen storage potential. The Teesside caverns are found to be smaller, flat and elliptical in shape, which makes them more useful for local end-use applications. For national, larger-scale storage purposes, caverns of these dimensions do not suffice, thus the research is focused on thicker salt beds in the UK. A similar study is performed by the Energy Technologies Institute, who identified several locations for UHS in the UK, and performed a short economic analysis on the different locations. It was concluded that a plant in Teesside, with smaller caverns, would need around 20 caverns to be able to fill a large gas turbine and a heat recovery steam generator, working at a load factor of 36%. Salt caverns in thicker salt formations will be larger and thus less are needed in a generation facility, which also has effect on the cost of the project (ETI, 2015).

The bedded salt formations in China have also been analysed for their energy storage potential (Peng et al., 2023). Several locations in China have been identified as potentially suitable, due to the proximity to wind and solar energy sources and the existence of salt mines in the area. Some of the present salt mining caverns have already been repurposed for gas or compressed air energy storage, however the majority of the caverns is not suitable for energy storage. This suitability is determined by the requirements for single-well-vertical (SWV) caverns, which are most commonly used to store gas. The SWV caverns are characterised by a single well and by having a significantly larger height than their width. The cavern requirements include a minimal salt formation thickness of 100 m, a depth of the formation of 400-1500 m, and minimal interlayers. Also no more than 20% of the total thickness should consist of interlayers and the salt should be of high grade, containing minimal insoluble matter (Peng et al., 2023). Peng et al., 2023 have proposed a two-well-horizontal cavern design, where the cavern is much wider than it is high, which makes it more suitable to thinner salt layers. This type of cavern has been found to be more suitable and profitable in bedded salt formations, creating and energy storage system with multiple alternate IE cycles and a high injection rate.

In Canada, Lemieux et al., 2019 analysed the UHS potential based on the formation properties and the proximity to major cities and renewable energy sources. The analysed salt formation is present on the land between

Lake Huron and Lake Erie, which is also in proximity to several major cities. A map showing the nuclear power plants and wind farms, also shows a clustering of these around the area of the salt formation. The paper concludes that this is a logical area for UHS in salt caverns, comparing the dimensions of such to the existing salt caverns in Teesside as the thickness of the salt formation is similar (Lemieux et al., 2019).

Bedded salt formations contain insoluble interlayers, which may have an effect on the stability of the salt cavern, this has been analysed by Zhang et al., 2021. When leaching the cavern, the interlayer content at the precise cavern location will be deposited as a sediment on the bottom of the cavern, effectively reducing the cavern volume. Thus, the usability of a salt cavern in a bedded formation with a high interlayer content has also been evaluated. When modelling the effect of a higher interlayer content, a few notable conclusions were made. Mainly, the stability of the cavern increases with the interlayer content, with the highest stability being at the highest interlayer content. The working volume of the cavern is lower with a higher interlayer content, but due to the increased stability there is more flexibility in the gas storage. To increase the working volume, the authors propose to enlarge the bottom of the cavern. Overall, the interlayer content had a positive effect on the cavern stability (Zhang et al., 2021).

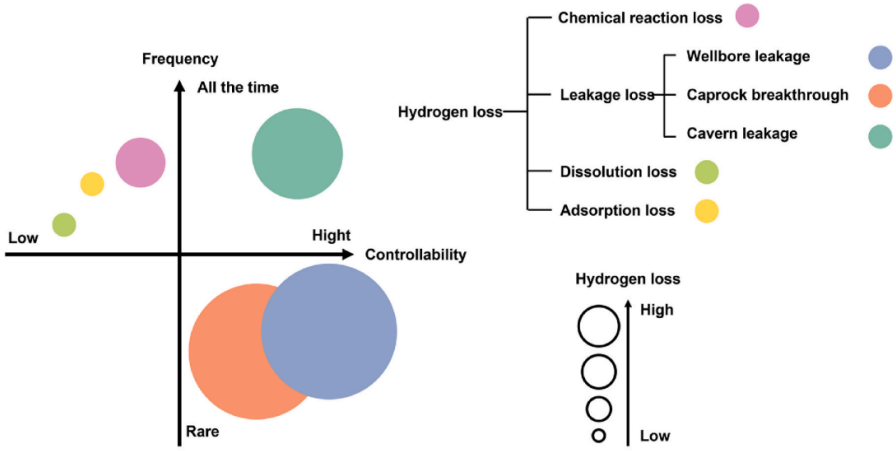

Figure 3. *Showing the frequency and amount of different hydrogen loss mechanisms in salt caverns (Zhu et al., 2023).*

Hydrogen has a low viscosity, small molecule size and contains active chemical properties, which lead to it being prone to reactions and losses within the storage mechanism (Liu et al., 2020). The types of losses experienced in bedded salt caverns and their frequency and amount are described

in Zhu et al., 2023. The results from the study are also shown in Figure 3. This figure shows that the most frequently occurring loss is through the interlayers in the cavern wall. However, the largest amount of loss experienced is through wellbore leakage and caprock breakthrough. The latter can be prevented through installing a safety roof of salt above the cavern top. Wellbore leakage can be reduced through proper and frequent maintenance of the equipment (Liu et al., 2020). The loss of hydrogen through interlayers has been further described by Liu et al., 2020 who have found that the cavern tightness can be ensured when the interlayer gas permeability is around $10^{-18}m^2$ or lower.

3 Methods

To answer the research questions, the research will be split into three main sections, each with its own results as described in Figure 4. The first section will identify the cavern and formation requirements for UHS and apply these to bedded salt formations. These values, along with values taken from literature, will then be applied to the model formed in the second section. The second section will focus on the creation of a hydrogen storage model in Python. The model will describe the simplified storage of hydrogen in a salt cavern with the dimensions found in the first section, adding more complex properties as the research furthers. The final section will translate the results of the model and literature research to the salt formations in the Netherlands, identifying possible storage locations and their storage potential.

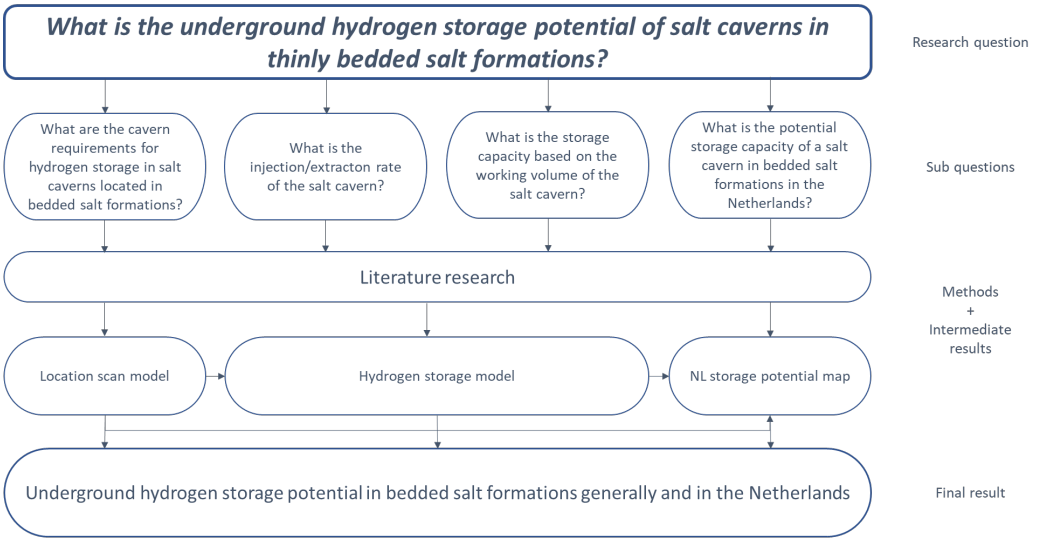

Figure 4. *Method structure of this research and the interactions between each research section.*

3.1 Cavern requirements in bedded salt formations

In order to identify the cavern requirements for UHS in thinly bedded salt formations, a literature study is performed. The requirements found are then used as boundary values for the first section of the model. This section of the model is named the Location Scan Model, and performs a first scan on the location values used as input. The model input values, salt formation depth and thickness, are entered through an excel file. The model

then uses the input data to calculate the cavern dimensions and checks these according to the formulated requirements. If these requirements are met, the cavern pressure range and the amount of hydrogen stored in the cavern are calculated. If the salt formation values are unknown, values from the existing UHS site in Teesside (UK) are used (Table 1). Finally, a diagram of the cavern with its requirements is given as output.

3.2 Hydrogen Storage Model

The IE cycles of hydrogen in a salt cavern will be modelled in a simple python model, which has been expanded upon throughout the research. The input data used will be specific to salt caverns in bedded salt formations. The cavern properties used as input will be taken from the Location Scan Model, as described in Section 3.1, or based on an existing UHS salt cavern in Teesside (Table 1). The model is outlined as followed; the input data is selected, hydrogen parameters are initialized, maximum injection and extraction velocities are set along with the corresponding flow rates, finally a dynamic section to the model is included to model the IE cycles over a set period of time. Within the dynamic model the cyclic loading profile of the cavern is adapted according to different pauses after a complete cycle. The dynamic model has also been adapted to allow for variable loading of the cavern, designing it to respond to an external energy demand/supply profile. All parameters used in the model that are not outlined in the text below, are given in Table A1.

3.2.1 Base model

Table 1. *Properties of the salt cavern in Teesside, UK (Williams et al., 2022)*

Location: Teesside, UK	
Properties	Value
Depth to cavern top (m)	450
Cavern height (m)	40
Cavern diameter (m)	70
Well inner diameter ($inch$)	7
Temperature of cavern ($^{\circ}K$)	300

A salt cavern will be assumed to be a cylinder, where the cavern walls are considered the boundaries, this due to their low porosity. Hydrogen will be injected and extracted through a single wellbore, of which the pipe

properties are taken from literature. A diagram of the proposed system is shown in Figure 5. Where h_{cavern} and d_{cavern} describe the height and diameter of the cavern respectively. P_{cavern} and T_{cavern} show the pressure and temperature in the cavern, which are assumed to be equal throughout the cavern. V_{cg} and V_{wg} describe the volumes of the cushion and the working gas inside the cavern. Finally, d_{pipe} is the inner diameter of the wellbore.

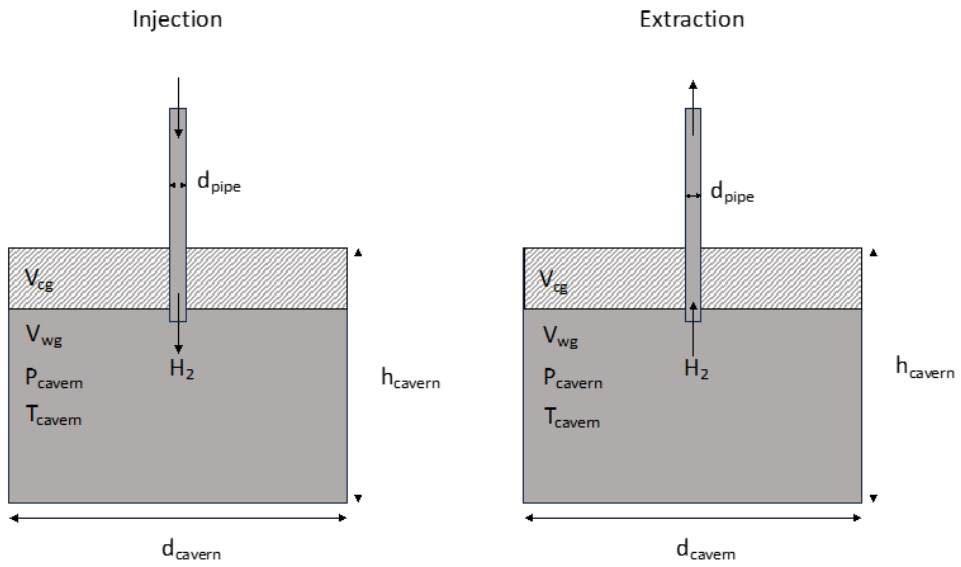

Figure 5. *A simplified diagram showing the injection and extraction of hydrogen in a salt cavern.*

The flow of hydrogen through the well is described using the ideal gas law:

$$Pv_{sp} = nRT \tag{1}$$

Where P is the cavern pressure (Pa), v_{sp} the specific volume of hydrogen stored (m^3), n the amount of hydrogen $(moles)$, R is the ideal gas constant $(8.314\ J/K * mol)$ and T the temperature (K). The ideal gas law can be used find the molar change and flow rate when injecting or extracting hydrogen in the cavern between the minimum and maximum operating pressures. This will be done under the assumption of constant volume and pressure.

The operating pressures are different per cavern, but certain limits are set to avoid significant subsidence and salt creep closing the cavern. The pressure range of the cavern should be between 30-80% of the overburden pressure (Equation 2), measured or calculated at the cavern roof (Thiyagarajan et al., 2022). Where $P_{overburden}$ is the overburden pressure in Pa,

using an overburden pressure gradient of 1 psi/m, which is converted to Pa/m. The depth to the cavern roof is given in m and is represented by D_{cavern}.

For simplification, the model will assume the cavern to be emptied to the minimum pressure before it is filled. However, this can be changed in the model to account for a more dynamic filling cycle. The literature also states that this cycle can be applied to salt caverns up to 10-12 times a year, which is also set as a boundary (Peng et al., 2023). The change in pressure is limited to a maximum of 1 MPa/day, which is similar to the pressure changes found in natural gas storage and will be used to find the maximum flow rates (Williams et al., 2022). These injection and extraction flow rates, $Q(m^3/day)$, can be found through Equation 3, where v is the flow velocity (m/s) and A_{well} is the inner area of the wellbore (m^2). For the flow velocities, the maximum values are set at 100 ft/s and 150 ft/s (converted to m/day) for injection and extraction respectively (Drnevich, 2014). In the model, a loop is created which runs through the velocities, calculating the flow rate until this reaches the maximum value, or until the maximum velocity is reached. This flow rate is converted to mass flow and energetic flow through Equation 4 and Equation 5; where $\dot{m}$ is the mass flow rate $(tonne/day)$, $\dot{E}$ the energetic flow rate (kWh/day), ρ_{H_2} is the density (kg/m^3) and LHV_{H_2} is the lower heating value of hydrogen (kWh/kg). The corresponding flow rates will then be used in the modelled IE cycles.

$$P_{overburden} = 22620.6[Pa/m] * D_{cavern} \tag{2}$$

$$Q = v * A_{well} \tag{3}$$

$$\dot{m} = Q * \rho_{H_2} \tag{4}$$

$$\dot{E} = \dot{m} * LHV_{H_2} \tag{5}$$

The hydrogen storage capacity is seen as the volume of the working gas in the cavern. There are certain ranges of cushion/working gas which have been given in literature as 20-30%/80-70% (Matos et al., 2019), or 30-40%/70-60% (Peng et al., 2023). Using this, the cavern working volume (m^3) is calculated through Equation 6, where $r_{cushiongas}$ represents the ratio of cushion gas to the total cavern volume. The working gas volume is assumed to be constant throughout the IE cycles. This volume is used, along with the minimum and maximum pressure, to find the upper and lower limits of hydrogen storage in the salt cavern using the ideal gas law.

$$V_{workinggas} = V_{cavern} - (V_{cavern} * r_{cushiongas}) \tag{6}$$

3.2.2 Dynamic model

The dynamic section of the model considers the IE cycles within the salt cavern. This is modelled over a set number of timesteps, for which the current mass is calculated in a for loop. Within this loop the status of the cavern is defined to either be extraction, injection or paused. The cavern starts in the extraction state, in which the cavern is emptied using the calculated extraction rate. Once the cavern content reaches the minimum value or below, it is set at the minimum value as a cavern content cap and the cavern enters the injection state. The cavern content is increased with the calculated injection rate. These changes in cavern content are modelled both in mass and energetic value. Once the cavern content has reached the maximum value or above, the cavern content is set as the maximum value and the cavern will enter the paused state or the extraction state, based on the pause type used. The paused state has been modelled in 3 variations: 1) A single pause; 2) Optimized pauses after each cycle; 3) Set pauses after each cycle. How each pause has been implemented will be described below. This pause, along with the minimum and maximum cavern content caps, are included to ensure the cavern is operated within the set safety boundaries for UHS facilities, as found in literature. The various pause options have been created to fit to different cavern situations. This way a long pause can be implemented for maintenance purposes once a year, or maintenance can be done after every cycle in a set or optimized number of days.

1) A single pause: The addition of a single pause has been introduced according to the cyclic loading cap, which is set at 12 in this research. Within the for loop, the number of cycles is counted once the cavern content reaches the maximum value. An if-statement is introduced which starts the paused state once the number of cycles has reached 12. The paused state keeps the cavern content constant at the maximum value. As it is written, the code employs the pause at the end of the year, but this can be modified by changing the starting date.

2) Optimized pauses after each cycle: The second pause option calculates the optimal number of pause days so that no more than 12 cycles will be run in a year (if a different number of maximum cycles is chosen, the model will run with that number). It does so by calculating the number of days it takes for a full cycle, and multiplying that by 12. This way the number of days which the loading should be paused is found. In the dynamic for loop, a pause state is reached after the injection phase. Here a pause counter, which is set to the optimal number of days, counts down to zero after which extraction will restart.

3) Set pauses after each cycle: The final pause option uses mostly

the same code as the second option with the addition of a few lines of code. It requires the user to fill in the number of paused cycle days. The code calculates the minimum number of days that the cyclic loading should be paused in order to not exceed the maximum number of cycles. This is done through an if statement before the dynamic section of the model, as in the second option. If a value is filled in which is too low, the model stops running and a prompt is given to fill in a higher number than the calculated minimum. Within the dynamic section of the model, the set pause days are implemented and plotted in the graph.

3.2.3 Variable loading

The dynamic model and pause variations described in Section 3.2.2 work from the main principle that the cavern will fully empty before it is filled. This fully emptying and filling of the cavern is considered a complete cycle. A salt cavern can also be used for short-term and variable storage amounts. This way it acts as a battery, being able to respond to a certain demand profile. To test how the addition of such a curve changes the loading profile the dynamic UHS model was adapted, creating a variable storage model.

Firstly, a demand profile was taken from the Energy Transition Model ("Energy Transition Model", n.d.). The profile chosen is the residual load curve of natural gas in the Netherlands in 2030. This profile is chosen as it gives a good overview of periods of energy shortage and surplus. The profile is an interpolation of current data which is used to estimate the residual load of natural gas in 2030. This profile is given in hourly data, which has been changed to daily averages to better fit the other data used and generated in this research. The curve has also been adapted to fit a multiple year simulation by simply assuming a similar pattern each year, which has been formed by copying the pattern for each new year. Below is a plot which shows the demand profile used over a period of 3 years.

The dynamic section of the model is written as follows. The same minimum and maximum values for energy and mass content are used as found in the base model. These form the bounds between which the cavern can be filled/emptied. The same IE rates as in the base model have also been used, which limit the amount of hydrogen injected and extracted per day. The dynamic loop runs over the simulation time and each demand profile value. A check is then performed, if the demand profile value is positive there is a shortage and the cavern status will be set to "extraction", in which the cavern content will be reduced by the extraction rate. A check will also be performed to make sure that the cavern content does not go below the

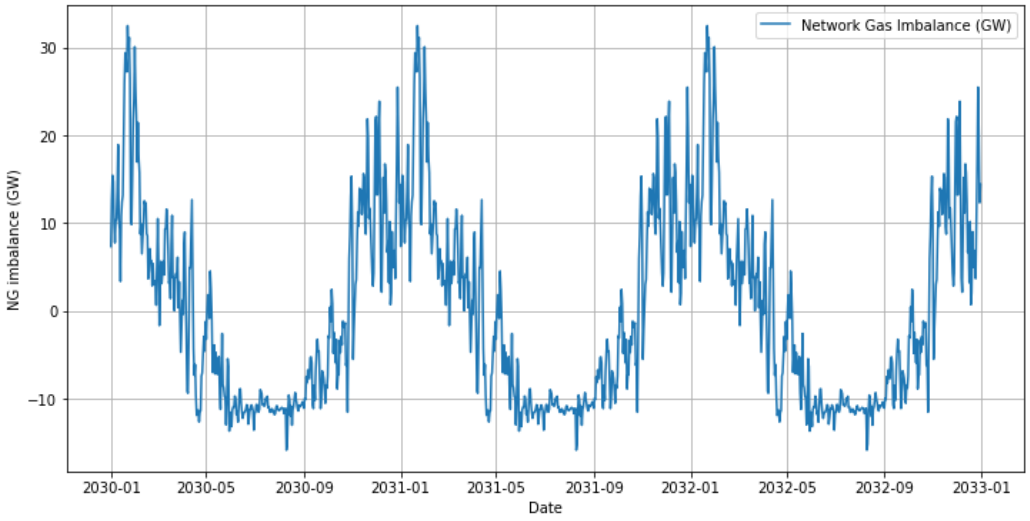

Figure 6. *The demand profile which is used in the variable loading section of the hydrogen storage model. The profile describes the residual load in 2030 ("Energy Transition Model", n.d.) and is modified to copy over the run time of the model.*

minimum value, and return it to this value if that is the case. If the demand profile value is negative, there is an energy surplus and the cavern status is changed to "injection", where the content in increased by the injection rate. A similar boundary check is performed using the maximum energy and mass content values. The loading profile data is saved and shown in a plot.

3.3 Storage potential in the Netherlands

The results from Section 3.1 and 3.2 will be gathered and then translated to a case study of the Netherlands. In this study, the bedded salt formations in the Netherlands will be analysed according to the salt formation depth and thickness at a certain location. This data will be gathered from borehole data which is publicly available through NLOG, and ordered in an excel file. This file is set up as shown in Table 2, where the column titles are shown along with the data source.

The location-specific values will be input for the Python model made, allowing for the calculation of the storage capacity and the storage properties of a cavern at that location. The output from the model will be translated into a map of the Netherlands, showing the analysed locations and the storage capacity in the country. This will be done in Python, as an added section to the model. The python package Folium is used to create an interactive map, on which each location will be shown with a pin. When clicking on this

Table 2. *Table showing the column titles and data sources used in the excel input file for the UHS model, which leads to a UHS potential scan of the Netherlands.*

Column title	**Data source**
Borehole ID	NLOG
Latitude	NLOG or map
Longitude	NLOG or map
Location	NLOG or own name
Depth (m)	NLOG
Thickness (m)	NLOG
Storage (GWh)	Hydrogen storage model
Injection rate (m^3/day)	Hydrogen storage model
Extraction rate (m^3/day)	Hydrogen storage model

pin, certain data is shown, namely the location, salt formation depth, salt formation thickness and the storage capacity.

Within the the Hydrogen storage model, the excel file is integrated through a for loop, which iterates over each location and calculates the storage properties for each location. This iteration also includes the creation of various diagrams and plots, which will be saved in the directory in folders named according to each location. The calculated values are also added to the original excel file, making it an input and output file.

4 Results and Discussion

The following section will describe and analyse the results from this study. Certain assumptions and limitations of the study are also noted in Section 4.4.

4.1 Cavern requirements

When considering UHS in salt caverns, there are certain design and safety criteria which are necessary or should be taken into account when designing such a storage location. Through literature research cavern requirements and design parameters were found, which are shown in Table 3. These were found in papers describing existing UHS caverns, caverns for UGS or computational models designing or testing caverns. The former is only found in papers which describe the UHS salt caverns found in Teesside, UK. The dimentions for these caverns are shown in Table 1, and used as a base case for the Location Scan and UHS models. Cavern dimension ranges and limits were identified through literature research on cavern design and safety criteria for UHS in specifically bedded salt formations. Research in salt diapers was not taken into account as the shape of caverns in these formations tends to be a vertically stretched ellipse, while caverns in bedded salt formations tend to take the shape of a horizontally stretched ellipse. In this research the cavern is modelled as a horizontally stretched cylinder, as mentioned in Section 3.

Table 3. *Cavern requirements as found through literature research. These values are used as input for the model.*

Parameters	**Value/range**
Casing shoe depth (m)	250-1800
Cavern height (m)	20-300
Cavern diameter (m)	70
Thickness of salt above (m)	20+
Thickness of salt below (m)	10
Pressure range	30-80% of $P_{overburden}$

Table 3 shows the boundaries which were found for the cavern dimensions. One note is that the cavern requirement model does not consider a range for the cavern diameter. The chosen value (70m) is the diameter of the caverns in Teesside. Through literature research the found cavern diameter

range is 60-100m. There is however no parameter in this model which can be used to base a diameter variation on. In practice, the cavern diameter can be varied based on the underground geological structures present. For instance, if there is a fault present in the area around the cavern location, a certain distance from the fault will be taken for safety measures.

When designing salt caverns for hydrogen storage, there are also certain pressure ranges which should be taken into account. Literature states that the pressure range which remains in the cavern should be 30-80% of the overburden pressure and that a fraction of the gas should remain in the cavern as cushion gas, as also explained in Section 3. These values and ranges are all taken as similar or equal to values currently used for storage of natural gas, either in reservoirs or salt caverns (Williams et al., 2022,Matos et al., 2019). The casing shoe maximum depth chosen is noted to be slightly conservative. The chosen range is taken from Williams et al., 2022 and is the standard range used for the casing shoe depth in natural gas storage caverns. The paper does note that the maximum depth is conservative, and that larger depths have been used for salt caverns created in other locations. It was chosen to continue with this maximum depth, as it is a boundary used in industry. The value can also be changed easily in the model if required.

The output of the literature research shows that there are two main limiting factors in the cavern design, which will likely also limit the suitability of salt formations in the Netherlands. The first limiting factor is the thickness of the salt which should be present above and below the cavern, which combined is 20+ m thick. There is a range in this value due to this range being present in the thickness of the salt layer above the cavern. In Williams et al., 2022 a distinction is made on this value based on the depth to the top of the salt layer. If the depth of the salt formation is under 250m, the casing shoe will be placed at 250m, and a 10m safety roof will be included under that. An example is seen in the image below (Figure 7), where the depth of the salt formation is 200m. The casing shoe is placed at 250m and the top of the cavern is at 260m. The total thickness of salt above the cavern is 60m in this example. If the depth of the salt formation is larger than or equal to 250m, the casing shoe will be placed 10m below the top of the formation, and the cavern top will be 10m below the casing shoe, so a total thickness of 20m will be present above the cavern top. This is seen in the right figure in Figure 7, where the depth of the salt formation is 500m, the casing shoe depth is 510m and the cavern depth is 520m, thus the total thickness of salt above is 20m.

Bedded salt formations are known to be thinner formations, which suggests that this will be a limiting factor in the size of the cavern possible and

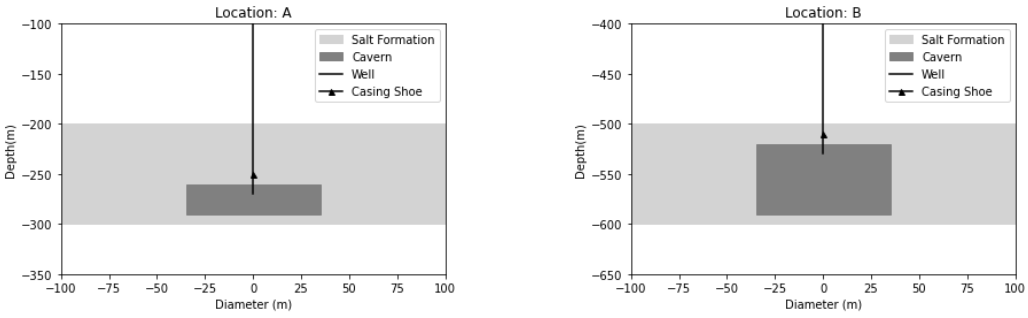

(a) *(b)*

Figure 7. *Two diagrams showing the difference in safety roof of the cavern. a) The casing shoe is placed at 250m, with a 10m safety roof above the cavern. b) The casing shoe is placed 10m under the top of the salt formation and 10m above the top of the cavern. Source: Location Scan Model.*

the overall possibility of forming a suitable cavern for UHS in various locations. Another limiting factor in the suitability of a location for UHS is the maximum depth of the casing shoe, which is 1800m. In some locations in the Netherlands, the depth to the top of the salt formation will be larger than this maximum, limiting the suitable cavern locations further. The maximum casing shoe depth of 1800m has been chosen as it is currently the maximum depth for casing shoes used in UGS facilities in the UK, however it is noted that this value is slightly conservative (Williams et al., 2022). Other literature uses a maximum depth of ca 1500-2000m, however there is no mention of a casing shoe here (Matos et al., 2019). When using the same logic as in Williams et al., 2022, the maximum casing shoe depth would come out to 1980m. It is noted that a larger depth is possible, however it would increase the cost of drilling and the risk of cavern closure due to the higher temperatures and overburden pressures (Matos et al., 2019).

The Location Scan model has an output of a diagram which shows the largest possible cavern available in this salt formation. Figure 8 shows the output of the model based on the data for the Teesside cavern in the UK. In this image it is seen that there is a layer of salt above and below the cavern, with the layer above containing the casing shoe.

One of the main assumptions made in the creation of this model, and the diagrams as shown above, is the continuity of the rock and salt layers. In reality there are many geological differences which can occur, even on a small scale, regarding the thickness and composition of the layers. For example, the salt layer could be 100m thick at the measured borehole location, but the thickness could reduce to 70m in a location 30m from the borehole. This would have implications for the dimensions of the salt cavern and the

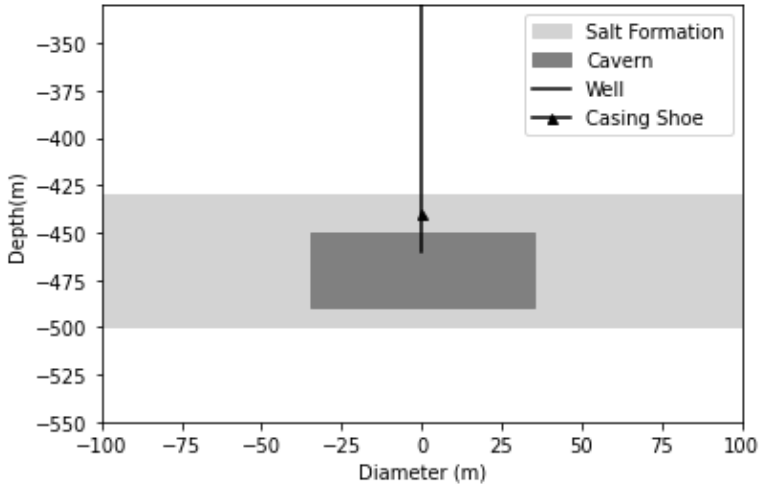

Figure 8. *Diagram of the largest possible cavern in Teesside, UK, as found in the Location Scan Model.*

storage capacity. As the caverns described are plotted over a distance of 70m, the chance that the layer thickness changes sufficiently is small. Thus for simplicity, the rock(salt) layers are assumed to be continuous.

4.2 Hydrogen storage model

The second, and largest section of this research has been developing and testing a python script which models the cyclic filling and emptying of a simplified salt cavern. This section will run through the different aspects added to the model and how the results changed with each model adaptation. The base model, as described in Section 3.2.1, sets the cavern dimensions equal to those found in Teesside (Table 1). Throughout this section the cavern in Teesside will be used as a reference case which allows for accurate comparison between each model adaptation and literature values.

4.2.1 Base model

The base model shows the cyclic extraction and injection of a salt cavern based on the dimensions of the caverns in Teesside. This model provides the basis of this study and complexities were added as the project evolved. The further subsections describe different alterations to the model or used parameters, and their influence on the model output.

Table 4 shows the main results from the base version of the hydrogen storage model. This model uses a cushion gas/working gas ratio of 30/70, a

well diameter of 7 inches and a maximum injection and extraction speed of 100 ft/s and 150 ft/s respectively. A complete cycle is seen as the emptying of the working gas and then filling the cavern with the same amount of gas. For the Teesside cavern, this process is completed within 135 days, which means that 2 full cycles can be completed in the time frame of one year.

The found storage capacity of the Teesside cavern is 14.66 GWh. When comparing this value to the values found in literature it is found to be in the same range. The caverns analysed in Williams et al., 2022 have a storage capacity of 158-176 GWh, however these caverns are located at a much higher depth. This depth allows for a larger amount of hydrogen stored due to the increase in density. The recorded value for the net storage capacity in the total Teesside cavern network is found to be 27 GWh (Crotogino, 2016). Considering this network is composed of three caverns, the capacity of a single cavern would be 9 GWh, which is smaller than the capacity found in this study. This difference is explained by the 9 GWh representing the net storage capacity, while this model does not incorporate conversion efficiencies. To give an indication of this storage size, the average household in the Netherlands uses 2479 kWh of electricity per year (Mileu Centraal, n.d.). Using this, the Teesside cavern modelled in this study would be able to supply 6631 households of electricity for a year. This value will in reality be lower as there are conversion losses when converting electricity to hydrogen and back into electricity.

Table 4. *Base model results using the cavern dimensions from Teesside as given in Table 1.*

Variable	**Value**
Extraction rate (m^3/day)	$9.81 * 10^4$
Injection rate (m^3/day)	$6.54 * 10^4$
Cavern working volume (m^3)	$1.078 * 10^5$
Cavern capacity (GWh)	14.658
Pressure range (MPa)	3.054 - 8.143
Time for one cycle ($days$)	134
Amount of cycles in a year	2

4.2.2 Well size

The IE rates (Equation 3) are determined by the IE velocity and the well area, which is calculated using the well diameter. Thus, the well diameter may be a limiting factor. To test this, the value has been adjusted to asses the

effect on the cavern cycles. When changing the diameter to 9 inches, which is what Juez-Larré et al., 2023 use in their model, the amount of completed cycles increases to 4, with a cycle taking 82 days. The injection rate increases to $1.08 * 10^5\ m^3/day$ and the extraction rate increases to $1.62 * 10^5\ m^3/day$. These values are around 60% larger than the IE rates found for the 7 inch well.

As this effect is sizable, the introduction of a second well has also been analysed, as is seen in Peng et al., 2023. For simplicity this second well will be modeled by changing the well diameter to two times the original well diameter, so 14 inches for a 7 inch well and 18 inches for a 9 inch well. The influence of the addition of a second well is seen in Figure 9. When adding a second well to the 7 inch system, the number of completed IE cycles increases to 10, which is five times higher than when operating with a single well. The change on the injection and extraction rates is also significant, with the values increasing to $2.62 * 10^5$ and $3.92 * 10^5\ m^3/day$ respectively. A similar trend is seen in the dual 9 inch well system, where the injection and extraction rates are respectively $4.32 * 10^5$ and $6.48 * 10^5\ m^3/day$. The number of IE cycles increases to 16 with the addition of a second well. The amount of cycles and the IE rates are all around four times the values found for the single well. This effect is expected as the IE rates are calculated using the well area, which is expressed by the well radius squared multiplied by pi.

4.2.3 Cyclic loading cap

The amount of cycles found for the two well simulation (18 inches) as described in the previous section results in 16 cycles per year. Literature states that a salt cavern used for UHS can undergo a maximum of 10-12 cycles per year, for it to retain its stability (Peng et al., 2023). To implement this as a boundary condition, a cyclic loading cap is set at 12 cycles, after which a pause is introduced. This results in a loading profile for a UHS cavern as seen above (Figure 10). This profile corresponds with a dual 9 inch well and runs over three years. The time taken per cycle is found to be 22 days, with the cyclic loading of the cavern being stopped after 264 days and restarted at the start of the new year. In this variation of the model, this loading pause is placed at the end of the year. This is done for simplicity reasons, but in principle these 101 days can be split between each of the cycles resulting in a pause time of approximately 8.5 days between each cycle. The spread of this pause can be implemented in any variation, as long as the cycle cap is still in place, as will be described in the following sections. An example of a single loading pause is also seen in a UGS project in the Netherlands, where the month of October is used for soaking of the depleted hydrocarbon reservoir

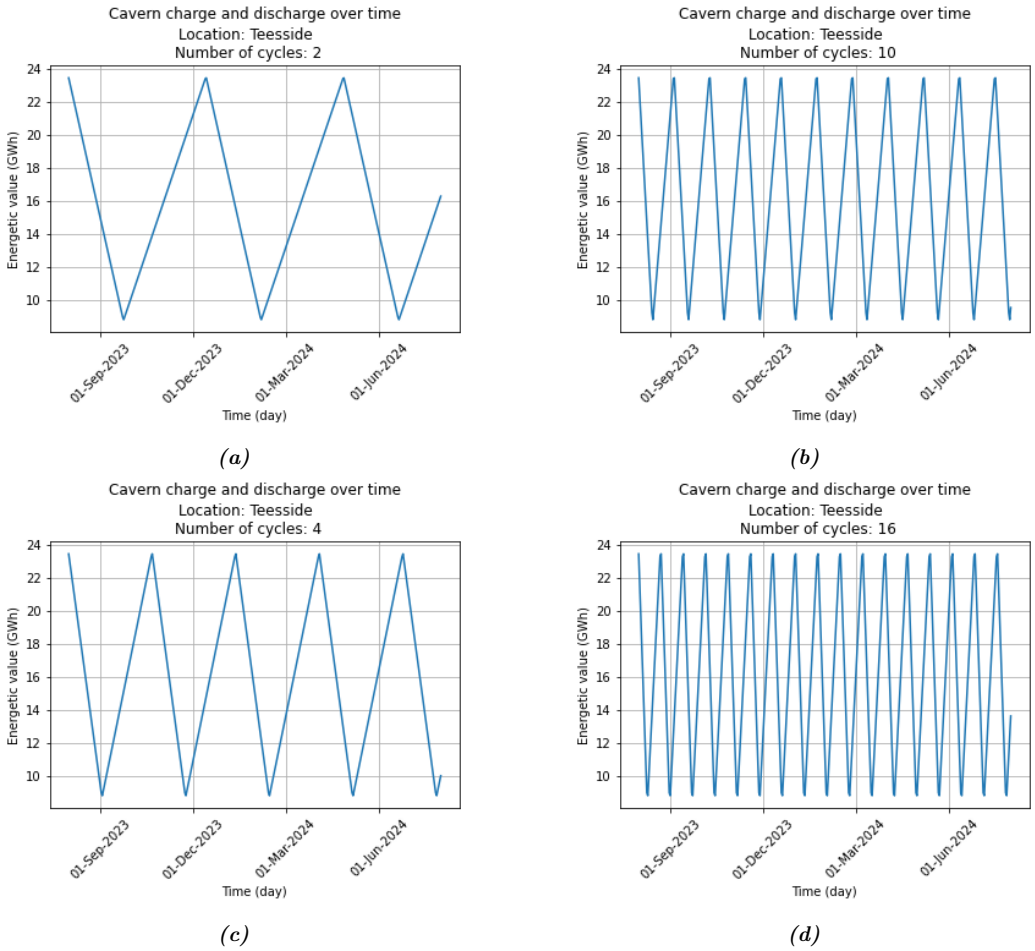

Figure 9. *The effect of adding a second well (through doubling of the well diameter) on the IE cycles over the period of a year, including the cyclic loading cap. Where a) Single 7 inch well, b) Dual 7 inch well, c) Single 9 inch well, and d) Dual 9 inch well.*

and maintenance of the plant (Yousefi et al., 2023). Such a use for the cyclic loading cap could also be implemented for UHS plants.

The implementation of a singular pause period may not match the use-case of some UHS plants. As described in Section 3, the other options developed in the model are an optimized pause time or a set pause time. These options allow for the varying of the cavern load profile to match the intended operational and/or maintenance periods. The optimized pause time is calculated based on the extraction and injection times, and when used returns a energy profile in which there is up to 12 cycles. Most runs end at 11 cycles per year, this due to the rounding up of the pause days in the model. This is done for simplicity as the cavern is modelled using days and

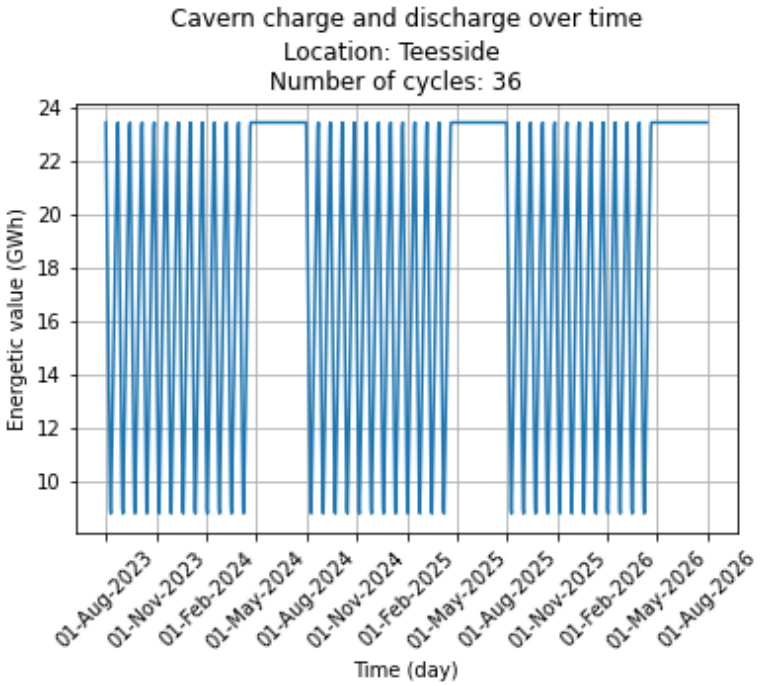

Figure 10. *Energy profile of the Teesside cavern with two wells, over three years.*

not hours. This also ensures that the cavern will never go over the maximum cycles, as it may when the number is rounded down. If the model is expanded to hours, the cyclic loading and pause times can be further optimized. These pause days allow for monthly maintenance, if there are around 12 cycles in a year.

If frequent maintenance is required, but the optimal pause days are too short, an alternate model has been developed which allows for a set amount of pause days. Figure 11 shows the effect of the difference in pause days on the energetic profile of the cavern in Teesside. The pauses are equally split over the model run time and allow for a constant pattern. The set pause is defined as 20 days in this run, which gives 10 extra days in between the cycles compared to the optimal pause simulation. This could allow for more flexibility around the maintenance or other operational processes.

The adaptation of the paused period to match maintenance periods allows for a certain assurance of safety of the storage site. One of the main concerns when storing hydrogen underground is the leakage potential, as described in Section 2.2. There are three main areas in which leakage can take place, through the interlayers in the evaporite layer, through caprock breakthrough, and at the well head. The former is discussed in Liu et al., 2020,

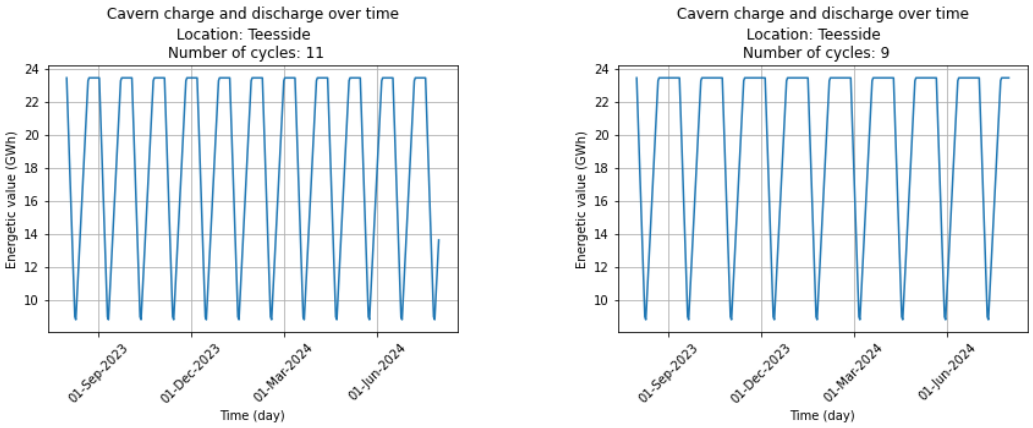

(a) *(b)*

Figure 11. *The effect of different pause options on the energetic profile of the Teesside cavern. a) Optimized pause for this cavern, calculated to be 10 days. b) Set pause, which is set at 20 days.*

who note that the tightness of the cavern is guaranteed with a maximum permeability of interlayers being $10^{-18}m^2$. The model described in the sections above does not take the occurrence of interlayers into account. The model will have to be altered to include interlayers and their composition. The permeability of the interlayers can then be used as a boundary condition for the size of the cavern.

Leakage at the well head is described in Zhu et al., 2023 and the effect and be reduced through proper monitoring and maintenance. Through the option of set pauses, such a maintenance period can be frequently introduced. The model created in this research shows a constant pause time over the run time of the model, however the model can be modified to include a pause time or pattern which best fits the maintenance time and schedule needed, which allows for a efficient operation while maintaining the safety of the storage site. An example of this could be that there is a longer pause added after two cycles, instead of a shorter pause after each cycle. Another option would be to take the single pause time and spread this over two larger pauses in the year.

4.2.4 Injection and extraction velocity

In the previous subsections it is noted that the IE rates were significantly affected by the well diameter. When looking at the equation used to find the IE rates (Equation 3) it is seen that the maximum IE velocities also have an effect on the IE rates. The velocities used in the base model

have been taken from literature, specifically a patent for a UHS salt cavern design (Drnevich, 2014). The values specified in this patent are a maximum injection velocity of 100 ft/sec and a maximum extraction velocity of 150 ft/sec, which translate to 30.5 m/s and 45.7 m/s respectively. The use of these speeds results in the loading curves seen in the previous sections.

During the base modelling the IE rates were found to be far under the maximum, which is set at $1.03 * 10^6$ m^3/day, thus some variations on the parameters well diameter and IE velocity were researched and applied. Juez-Larré et al., 2023 used maximum IE velocities in their gas storage model, which both have a value of 100 m/s. These speeds are 2-3 times higher than those noted in the patent. Figure 12 shows the effect of the different IE velocities on the cavern loading curves with two different pause options, with the system considering a dual 9 inch well. When comparing the two loading profiles with the single pause, it is seen that the pause is much longer when the larger IE velocities are used. The pause time more than doubles from 101 days to 221 days. This increase of paused days is also seen in the optimal pause run, where the optimal time with the IE velocities noted in Drnevich, 2014 is 10 days. When using the IE velocity times found in Juez-Larré et al., 2023, the amount of paused days increases to 20 days. This amount also increases the minimum pause time in the set pause model to 20 days.

The single pause, optimal pause and set pause time all have the same IE rates as the only difference in the modelling is the distribution and length of the pauses. Through the increase in IE velocity, the IE rates are set at $1.03 * 10^6$ m^3/day for a dual 9 inch well, which corresponds to the maximum value of 1 MPa/day. This maximum value is also reached when using the dual 7 inch well system.

Figure 12 shows that the IE velocities from Juez-Larré et al., 2023 significantly decrease the cycle time in a dual-well system from 21 to 11 days. As noted in a previous section, the well diameter was a limiting factor for the amount of IE cycles in a year. The results above show that by increasing the IE velocity, the cycle time is reduced by about 48%, which may allow a single-well cavern to reach more completed cycles per year. To test this, the same models and variations are run as in Figure 12, but with a single well. These results are shown in Figure 13. When increasing the IE velocities, the number of completed cycles increases from 4 to 11 or 12, depending on the model type used. This corresponds to a cycle time of 30 days for a single 9 inch well system, which is a 63.4% decrease. The IE rates found for this system are $3.55 * 10^6$ m^3/day, which is comparable to the values found for the 7 inch dual-well system. This IE rate is lower than the maximum IE rate corresponding to 1 MPa/day, which has been reached with a dual well

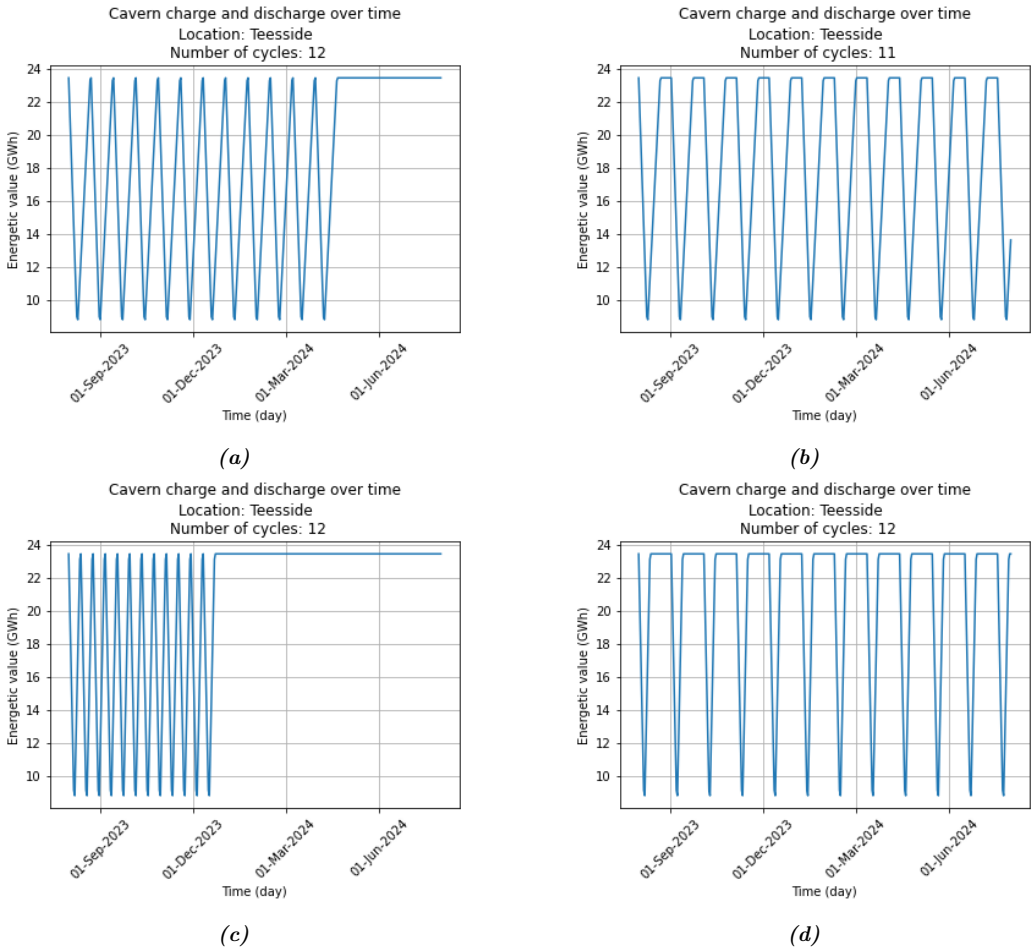

Figure 12. *The use of different IE velocities on the loading curve of the Teesside cavern with two 9 inch wells (model well diameter=18 inches). a) IE velocities found in Drnevich, 2014 with a single pause. b) IE velocities found in Drnevich, 2014 with the optimal pause time. c) IE velocities found in Juez-Larré et al., 2023 with a single pause. d) IE velocities found in Juez-Larré et al., 2023 with the optimal pause time.*

system.

When comparing the diagrams a) and b) in Figure 13, a difference is seen in the loading curve at the end of the runtime. In the single pause model there is a slight injection at the end of the year, while this is missing in the optimal pause day. This small discrepancy is likely due to the difference in code used for each model. A difference in loading curve is also seen in diagrams c) and d). When increasing the IE velocities in the single pause model, 12 cycles are completed and a pause of 5 days is included at the end of the year. When looking at the model with optimal pauses, 11 cycles are completed. In this model the 5 pause days are spread between the cycles,

which would amount to 0.45 days between each cycle. The optimal pause model is set to round up the paused period to a day. This is done as the data input is daily values. When not rounding the values, the maximum amount of cycles was found to be surpassed in some model runs, thus crossing the boundary condition of the model. This rounding results in a pause time of 1 day and a total of 11 completed cycles in a year.

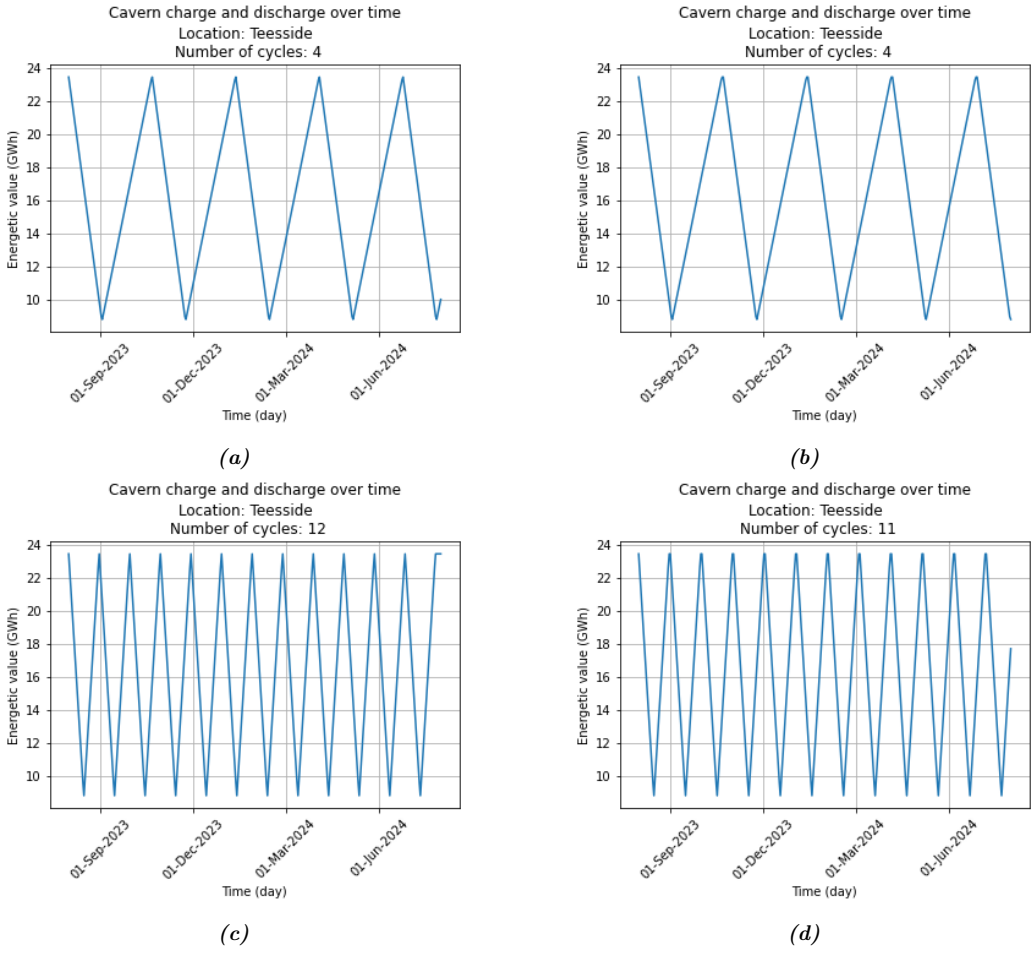

Figure 13. *The use of different IE velocities on the loading curve of the Teesside cavern with a single well (well diameter=9 inches). a) IE velocities found in Drnevich, 2014 with a single pause. b) IE velocities found in Drnevich, 2014 with the optimal pause time. c) IE velocities found in Juez-Larré et al., 2023 with a single pause. d) IE velocities found in Juez-Larré et al., 2023 with the optimal pause time.*

The values found in this study should be comparable to the values found in other studies modelling the storage of hydrogen in salt caverns. In Williams et al., 2022 various locations have been analysed for their UHS potential in salt caverns. In this study the values found for the cycle time

are more comparable to the values found when using a double well or the IE velocities found in Juez-Larré et al., 2023. The cycle times found in Williams et al., 2022 range from 18 to 26 days, for caverns at a depth of 1200+ m and with capacities of 158-176 GWh. The cavern analysed in this study is much smaller at 14.66 GWh and at a more shallow depth of 450m. The cycle time for this cavern ranges from 11 days when using a dual-well to 30 days when using a single well. IE velocities are set at 100 m/s in these simulations. The calculations in Williams et al., 2022 make use of a single well, which when compared to the single well simulation in this study, have a slightly faster cycle time, however the values are in the same range.

The cycle times found in Williams et al., 2022 are most comparable to the 100 m/s IE velocity results, which suggests that these values are most in line with the values found in literature. A smaller IE velocity, like the one used in Drnevich, 2014, can be considered when using a smaller cavern, or when wanting to deploy a dual well. In this case the smaller IE velocity will lead to a longer cycle time and thus potentially a more even spread of cycles over the year.

4.2.5 Variable loading

The model and analysis described above assumes that the salt cavern is either used for seasonal storage, with certain paused time frames, or constant cyclic loading. To test the use of a salt cavern with variable loading, the cavern was modelled similar to a battery, as described in Section 3.2.3. This model can also be run with other loading profiles, as will be described further in the following section. All figures below are run with a single 9 inch well. This was chosen as the values are found to be most comparable to those in literature.

The variable loading profile of the Teesside cavern over a period of 3 years, starting in 2030 is shown in Figure 14. The demand profile generally shows a surplus in the summer months and an energy shortage in the winter months (northern hemisphere). This pattern is reflected in the loading profile of the cavern. When looking at a single year of the pattern, the cavern has short periods of extraction and injection. The rest of the year consists of the cavern content either being at the maximum or minimum values, which for this cavern are at 8.79 and 23.45 GWh. The cavern is also not able to supply or store the total values of energy shown in the demand profile. This may be solved by introducing a network of caverns or a larger cavern. The current caverns deployed in Teesside form a network of 3 caverns. This is also seen in the USA, where the three caverns in salt domes in Texas are connected through a pipeline, forming a network of UHS caverns (Crotogino, 2022).

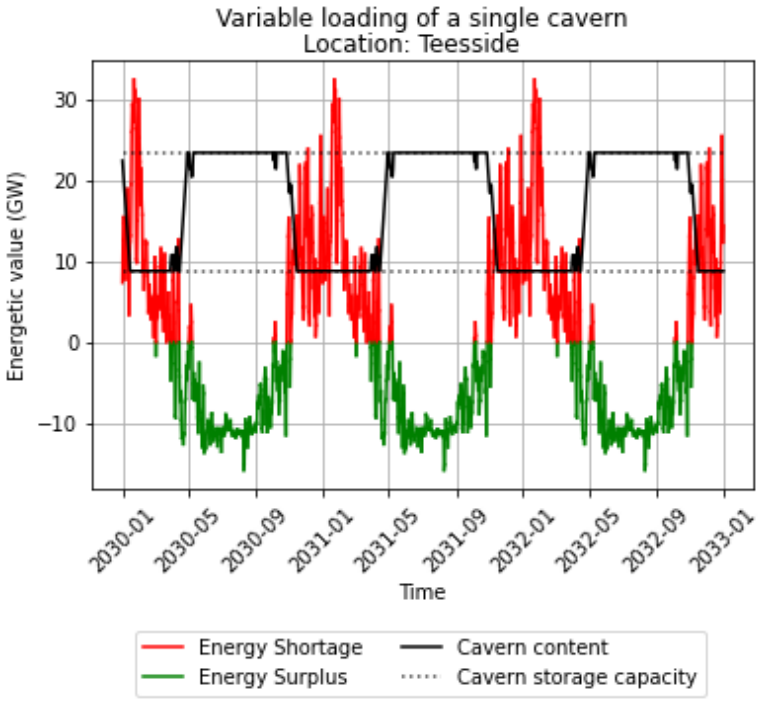

Figure 14. *Cavern loading profile of the Teeside cavern when using variable loading (black). The red and green lines describe the demand profile used in the simulation, with the green representing and energy surplus and the red representing and energy shortage. The dotted lines represent the boundaries of the storage capacity of the cavern.*

The demand profile used in this study (Figure 6), describes the network gas imbalance in 2030 in the Netherlands. As described above, the values in this demand profile are significantly larger than the storage capacity of the cavern. It would be interesting, for future research, to run the variable loading model using the demand curve of a certain city or town. This way the local use of a cavern can be analysed. It is to be noted that the daily increase or decrease in cavern content is set as the IE rates (Section 3.2.3). The IE rates are capped corresponding to the maximum of 1 MPa/day, which corresponds to a energetic value of 2.9 GWh/day. This shows that the cavern will not be able to supply a daily energy shortage of 30 GWh a day, as is shown in Figure 6. This maximum IE rate is described in literature and used to adhere to certain safety standards. Through employing a network of caverns the storage capacity needed for such a residual load profile can be reached.

4.3 Case study: the Netherlands

This section describes the results gathered when using the models described in the previous sections to analyse the UHS potential in the Netherlands. Various locations in the Netherlands haven been chosen according to the presence of bedded salt formations, as seen in Figure 2.

4.3.1 Storage map

The final output of the python model consists of an interactive map, showing the storage characteristics of single caverns at various locations in the Netherlands. The map created in python allows for a quick scan of various possible locations. The locations chosen in this study have been chosen on a few basic criteria namely, the general location of salt deposits in the Netherlands and the depth of these deposits. As noted previously, the main locations where salt deposits are found is in the North and East of the Netherlands. This map also shows salt deposits in the West of the Netherlands, however these are identified as relatively thin and some formations are also located at a depth which is larger than the maximum casing shoe depth. As mentioned in Section 4.1, the maximum value chosen can be conservative, thus the increasing of this value could increase the suitable areas in the Netherlands.

The chosen boreholes and the corresponding data found in NLOG, has been used as input for the model. This input file is designed as easy to use and will therefore also be open to user input. This way users can focus on a specific area of the Netherlands, in which the hydrogen storage potential can be analysed. Figure 15 shows a screenshot of the map generated through running the model with the chosen boreholes, of which an overview of the found input data is given in Table 5.

The image above shows the map which is given as output by the model. The map allows the users to click on each borehole site to show more information on the storage properties of a single borehole at each locations. There are three locations are highlighted in this image; Weerselo, Steenderen and Biddinghuizen. The storage capacity is largest in Steenderen, and lowest in Biddinghuizen. This is defined by the depth and thickness of the layers, which influences the size of the cavern and the cavern pressure. This influence can clearly be seen in the examples given. The Steenderen cavern is at a large depth, which increases the cavern pressure. The density of hydrogen increases with pressure, thus there will be a larger hydrogen content at a larger depth.

The Weerselo cavern is located at a much lower depth than the Steen-

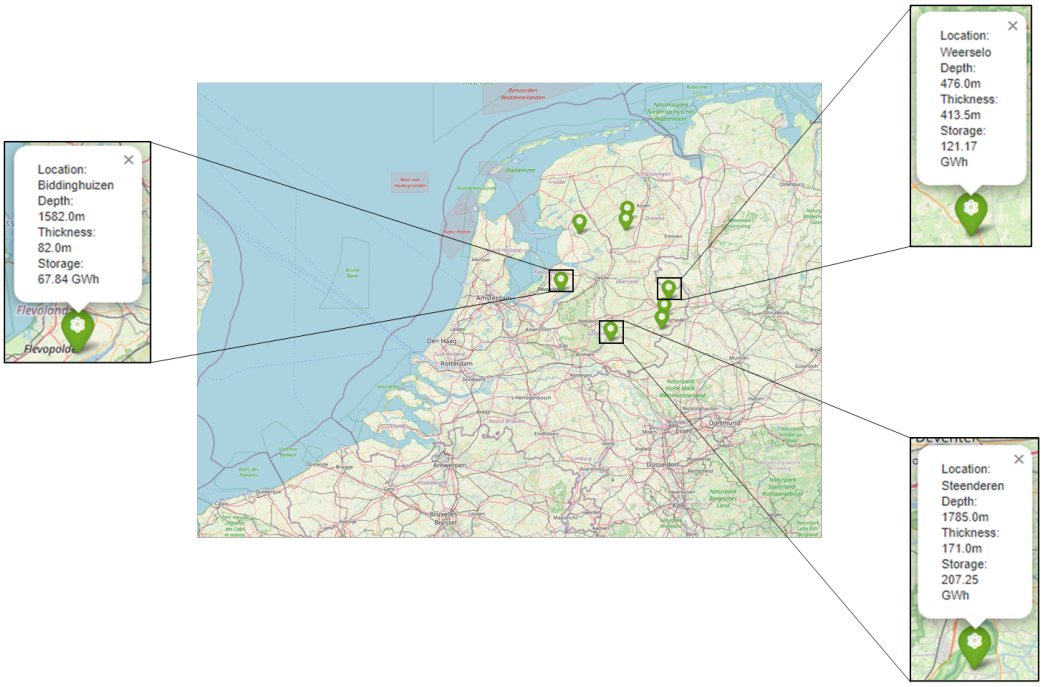

Figure 15. *An overview of the map generated within the model. Each of the green pins represents are borehole which is used for input data. The image also shows certain data which is included on the map for each location.*

deren cavern, namely 476m instead of 1785m. The evaporite layer is 413.5m thicker compared to the 171m in Steenderen. This larger layer thickness allows for a much larger cavern, and thus a larger storage potential.

The Biddinghuizen location has the smallest storage potential of the three, 67.84 GWh, which is due to the layer thickness being 82m. This evaporite layer thickness is more comparable to that of the Teesside location. Here the evaporite thickness is 70m and the depth is 430m. However the storage potential in Teesside is 14.66 GWh, which is significantly lower than the capacity calculated for Biddinghuizen. This difference is due to the higher depth at which the Biddinghuizen cavern is located, namely 1582m compared to 430m in Teesside.

The results described above show the effect of evaporite layer thickness and the evaporite depth on the hydrogen storage capacity of a single salt cavern. As seen in Figure 15, there are more locations than the ones mentioned above. Table 5 shows the information shown on the pop-ups in each location on the map, including the locations discussed above.

Table 5. *Table showing the results shown on the map for each potential UHS storage site which has been run through the model. The Teesside location is included as it is the base case in this study. Using a well diameter of 9 inches and IE velocities of 100 m/s.*

Location	**Depth** (m)	**Thickness** (m)	**Storage** (GWh)	**Cycle duration (days)**	**Pressure range (MPa)**
Teesside	430.00	70.00	14.66	30.00	3.05 - 8.14
Biddinghuizen	1582.00	82.00	67.84	138.00	10.87 - 28.99
Dwingeloo	1384.00	235.00	234.38	474.00	9.53 - 25.41
Haaksbergen	699.00	131.00	59.13	120.00	4.88 - 13.01
Hengelo	323.50	60.70	8.59	18.00	2.33 - 6.22
Hoogersmilde	1746.00	168.00	198.45	401.00	11.98 - 31.96
Slijkenburg	1765.00	140.00	159.89	324.00	12.11 - 32.30
Steenderen	1785.00	171.00	207.25	419.00	12.25 - 32.66
Weerselo	476.00	413.5	121.17	245.00	3.37 - 8.98

4.3.2 Variable loading

In Section 4.2.5 the variable loading model has been introduced, along with the results for the Teesside cavern. This cavern was found to be relatively small and not able to balance the total capacity of the residual load. In Table 5, various caverns with a larger storage capacity are seen. Thus, the variable loading model has also been run for the locations Haaksbergen and Weerselo (Figure 16).

In Figure 16, the variable loading profiles for single caverns in Haaksbergen and Weerselo are shown. When comparing the two diagrams, there are a few noticeable differences. The first is that the cavern storage values in Weerselo are almost double those found in Haaksbergen. This is also seen in the values in Table 5. The other difference is that the time that the cavern spends at minimum or maximum capacity is smaller for the Weerselo cavern than for the Haaksbergen cavern. The Weerselo cavern plot does not completely go to minimum in the first and last year of the simulation, which is interesting. If the demand profile is similar in the periods of shortage and surplus every year, the cavern will go to minimum. If the variable load was to be plotted over a year, the cavern would be able to supply hydrogen in times of shortage. However as the shortage period continues in a new year, this is not the case.

When comparing the two cavern plots to Figure 14, the variation in

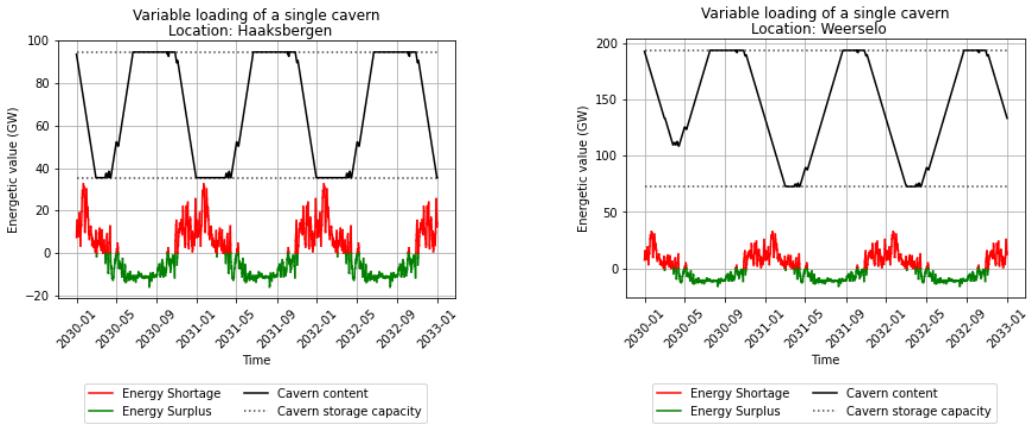

(a) *(b)*

Figure 16. *The variable loading profiles of a single cavern in a) Haaksbergen and b) Weerselo.*

time spent at minimum/maximum capacity is reflected. The Teesside cavern has the largest amount of time spent at minimum/maximum capacity. The time spent at these values is the times at which the cavern cannot store or deliver hydrogen. Thus, a long time spent at these boundary values suggests that the cavern is not able to meet the demand of the area which the profile reflects. Adding to this that the IE rates are capped at a maximum of 2.9 GWh/day, the same is seen as in Section 4.2.5. From this interpretation, all three caverns discussed in this section are not able to meet the residual load demand of the Netherlands in 2030, as displayed in the profile used. The caverns shown are all single caverns, so a network of various caverns could meet the residual load demand. By increasing the amount of caverns above this residual load capacity, there will be excess capacity free. This capacity can be filled with excess hydrogen which can be used for international trade, adding to the economy of the Netherlands.

4.4 Assumptions and limitations

In this study a model has been created which allows for the quantification of the storage potential in various bedded salt formations. This is done through the simplification of various processes and through the use of certain assumptions, which will, along with the limitations of this study, be summarized and discussed below.

The first assumptions made are those regarding the geological composition of the area. As discussed in Section 4.1, the continuity of the rock layers and their composition is assumed. In reality these may differ over the

distance, and certain other geological formations such as faults can occur. The presence of interlayers was also not taken into account in this study. The research done by in Liu et al., 2020 and Zhang et al., 2021 shows that the presence of interlayers has an effect on the hydrogen leakage and the stability of the cavern. The assumptions made have allowed for an analysis of the theoretical potential of hydrogen storage in salt caverns in various locations. To find the technical potential of UHS in salt caverns, certain values and techniques will have to be included, such as the geology of the area.

Another important assumption made, which limits the accuracy of the found storage characteristics, is that hydrogen is considered as an ideal gas. Along with this, it is also assumed that the temperature and pressure are constant within the cavern. The temperature is also set at 300 K, for all model simulations, meaning that the effect of temperature on the storage potential has not been analysed. Zhang et al., 2021 has shown the effect of interlayer content on the volume shrinkage of salt caverns. In this study the volume shrinkage was assumed to be zero. In reality, hydrogen will not act as an ideal gas, and there may be an effect on the storage capacity due to pressure and temperature changes in the cavern. Further research needs to be done to account for these parameters in such a model.

The hydrogen storage model as described in this study does not include hydrogen transport to the wellbore and the surface processes included. The amount of hydrogen extracted or injected into the cavern is the value taken at the wellhead, before or after any surface processes which may lower or increase the amount of hydrogen which enters the surface system. It would be interesting to be able to model the entire path of hydrogen movement through the system, which will be a task for further research. This way other potential hydrogen loss areas can be identified and the total energy input of the storage process can be quantified.

5 Conclusion

This study has evaluated the underground hydrogen storage potential of thinly bedded salt formations. The research has been split into three main sections, each answering their own research questions, as outlined in Figure 4.

The first section describes the cavern requirements for a UHS cavern in bedded salt formations. There are various requirements for UHS in general, mainly to ensure the safety of the storage site and to minimize the hydrogen loss through leakage. The main requirements used in this study are related to the cavern depth and the thickness of the evaporite layer. The maximum depth considered in this study is slightly conservative, but in line with the UGS requirements in the UK. The operating pressure range in the cavern has also been found through literature research to be dependant on the overburden pressure, which is calculated according to the cavern depth. In literature certain properties regarding the interlayer content and its composition were found, however these were not included in the created model. To answer the first subquestion, a model was created in which depth and layer thickness is used as input. This then runs through the found cavern requirements, resulting in a diagram of the largest possible cavern and its dimensions. Through this tool a first identification of the potential for UHS can be identified and visualized.

The second section of the research focused on the answering of the second and third subquestion through a python model of the cyclic injection and extraction of hydrogen in a salt cavern. This model describes a cylindrical cavern, in which hydrogen acts as an ideal gas. This model was adapted during the research, which is well described in Section 3 and 4. The first adaptations were the increase of the well size from 7 to 9 inches in diameter, and the introduction of a dual-well system. This adaptation lead to larger IE rates, as these are dependant on the well size and IE velocities. To test the influence of the latter, larger IE velocities were taken from literature. The single well systems run with these speeds had similar IE velocities to the dual-well systems with the lower speeds. Overall, the introduction of a second well or larger velocities both have their advantages. The choice between the two, or including both in a system will be made according to the use-case of the cavern.

Another modification to the second model was the introduction of a loading cap, set at 12 cycles per year, and the different spreading of pauses. The loading cap did not have an influence on the low IE velocity, single well systems as these did not reach 12 cycles. The higher velocity and dual well

systems are impacted by the loading cap. The loading cap halts the injection and extraction for a series of time. This time is either spread in between the cycles, or kept as one longer pause period. The choice for a singular pause or multiple pauses can be made according to the required cavern maintenance. The multiple pauses offers the chance to have frequent short maintenance periods, however a single pause period allows for one longer maintenance period.

Overall the second model gives an overview of the storage system over a year. The storage capacity is calculated based on the working gas/cushion gas ratio, which is set at 70/30. This leads to a cavern storage capacity of 14.66 GWh for the modelled cavern in Teesside, which is in line with the values found in literature. This storage capacity is enough to power 6631 average Dutch households for a year. Based on the use-case of the storage system, choices can be made for single or dual well systems, the spreading of the pause time and the length of the pause time. Further research should be done to model the storage system for a real gas and varying cavern shapes, pressures and temperatures.

The third section of this study focuses on the storage potential in the Netherlands. To test this a section was added to the model, which takes borehole data as input and outputs an interactive map showing the storage capacity of a single cavern at a given location. The model also creates loading profiles and cavern diagrams for each location. This provides a basis on which potential storage locations in the Netherlands can be compared. Overall, the model shows that there are various locations which provide suitable large-scale storage sites. Many smaller caverns are available in bedded salt formations, which could be sufficient to be used as a local storage site for a city or town. Furthermore the use of multiple caverns could provide excess storage space, which can be used for international trade and connected through an international hydrogen network. The design and specifics of these use-cases should be outlined in future studies. It would also be interesting to compare the costs of different sizes of caverns.

Acknowledgements

I wish to extend my gratitude to all the people who have made my research possible. Firstly I want to thank Hamed Aslannejad for the frequent meetings, support and feedback throughout the entire process. Secondly I want to thank Antea Group for giving me the opportunity to work on this project specifically and for the freedom in the formulation of my research aim. I specifically thank Søren Winkel and Sander Turk-van Utrecht from Antea Group, who have helped me when formulating my research aim and questions, and during the creation of my python model. Lastly I want to thank my family an friends for their emotional support throughout my research and writing process.

References

Abreu, J. F., Costa, A. M., Costa, P. V., Miranda, A. C., Zheng, Z., Wang, P., Goulart, M. B., Bergsten, A., Ebecken, N. F., Bittencourt, C. H., Assi, G., Meneghini, J. R., & Nishimoto, K. (2023). Large-scale storage of hydrogen in salt caverns for carbon footprint reduction. *International Journal of Hydrogen Energy*, *48*(38), 14348–14362. https://doi.org/10.1016/j.ijhydene.2022.12.272

Altenburg, R. (2022). Storage and disposal potential of the Triassic Röt Formation in the east of the Netherlands: Subsurface mapping and facies interpretation.

Brunner, L., Díez, N. G., & Dijkstra, H. (2022). Hy3-Large-scale hydrogen production from offshore wind to decarbonise the Dutch and German industry. Feasibility study Hy3.

Caglayan, D. G., Weber, N., Heinrichs, H. U., Linßen, J., Robinius, M., Kukla, P. A., & Stolten, D. (2020). Technical potential of salt caverns for hydrogen storage in Europe. *International Journal of Hydrogen Energy*, *45*(11), 6793–6805.

Crotogino, F. (2016). Chapter 20 - larger scale hydrogen storage. In T. M. Letcher (Ed.), *Storing energy* (pp. 411–429). Elsevier. https://doi.org/https://doi.org/10.1016/B978-0-12-803440-8.00020-8

Crotogino, F. (2022). Large-scale hydrogen storage. Elsevier.

Crotogino, F., Donadei, S., Bünger, U., & Landinger, H. (2010). Large-Scale Hydrogen Underground Storage for Securing Future Energy Supplies. *Proceedings WHEC*.

Drnevich, R. F. (2014, June). Hydrogen storage method and system.

Energy Transition Model. (n.d.). Retrieved January 8, 2024, from https://energytransitionmodel.com/

ETI. (2015). Hydrogen: The role of hydrogen storage in a clean responsive power system. an insight report by the energy technologies institue.

European Council. (n.d.). Fit for 55. https://www.consilium.europa.eu/en/policies/green-deal/fit-for-55-the-eu-plan-for-a-green-transition/

Gasunie. (n.d.). Project: Waterstofnetwerk Nederland. https://www.gasunie.nl/projecten/waterstofnetwerk-nederland

Groenenberg, R. M., Juez-Larre, J., Machado, C. G., Wasch, L. J., Dijkstra, H. E., Wassing, B. B. T., Orlic, B., Brunner, L. G., van der Valk, K., & van der Meulen, T. C. H. (2020). Techno-economic modelling of large-scale energy storage systems.

Hematpur, H., Abdollahi, R., Rostami, S., Haghighi, M., & Blunt, M. J. (2023). Review of underground hydrogen storage: Concepts and challenges. *Advances in Geo-Energy Research*, *7*(2), 111–131.

Hydrogen TCP-Task 42. (2023). *Underground Hydrogen Storage: Tehcnology Monitor Report* (tech. rep.). https://filelist.tudelft.nl/Websections/H2%20platform/Task42%7B%5C_%7DUHS%7B%5C_%7DTechnologyMonitoringReport.pdf

HyStock. (n.d.). HyStock. Retrieved October 13, 2023, from https://www.hystock.nl

Juez-Larré, J., Gessel, S. V., Dalman, R., Remmelts, G., & Groenenberg, R. (2019). Assessment of underground energy storage potential to support the energy transition in the Netherlands. *First Break*, *37*(7), 57–66.

Juez-Larré, J., Gonçalves Machado, C., Groenenberg, R. M., Belfroid, S. S., & Yousefi, S. H. (2023). A detailed comparative performance study of underground storage of natural gas and hydrogen in the Netherlands. *International Journal of Hydrogen Energy*, *48*(74), 28843–28868. https://doi.org/10.1016/j.ijhydene.2023.03.347

Lemieux, A., Sharp, K., & Shkarupin, A. (2019). Preliminary assessment of underground hydrogen storage sites in ontario, canada. *International Journal of Hydrogen Energy*, *44*(29), 15193–15204.

Liu, W., Zhang, Z., Chen, J., Jiang, D., Wu, F., Fan, J., & Li, Y. (2020). Feasibility evaluation of large-scale underground hydrogen storage in bedded salt rocks of china: A case study in jiangsu province. *Energy*, *198*, 117348.

Małachowska, A., Łukasik, N., Mioduska, J., & Gbicki, J. (2022). Hydrogen storage in geological formations—The potential of salt caverns. *Energies*, *15*(14), 5038.

Matos, C. R., Carneiro, J. F., & Silva, P. P. (2019). Overview of large-scale underground energy storage technologies for integration of renewable energies and criteria for reservoir identification. *Journal of Energy Storage*, *21*, 241–258.

Mileu Centraal. (n.d.). Gemiddeld energieverbruik. Retrieved January 23, 2024, from https://www.milieucentraal.nl/energie-besparen/inzicht-in-je-energierekening/gemiddeld-energieverbruik/

Ministry of Economic Affairs and Climate. (2020). *Government Strategy on Hydrogen* (tech. rep.). https://www.government.nl/documents/publications/2020/04/06/government-strategy-on-hydrogen

NLOG. (n.d.). Steenzout. Retrieved November 29, 2023, from https://www.nlog.nl/steenzout#:~:text=De%20belangrijkste%20steenzoutvoorkomens%20in%20onze,in%20ondiepe%2C%20deels%20afgesloten%20zoutmeren.

Papadias, D., & Ahluwalia, R. (2021). Bulk storage of hydrogen. *International Journal of Hydrogen Energy*, *46*(70), 34527–34541. https://doi.org/10.1016/j.ijhydene.2021.08.028

Peng, T., Wan, J., Liu, W., Li, J., Xia, Y., Yuan, G., Jurado, M. J., Fu, P., He, Y., & Liu, H. (2023). Choice of hydrogen energy storage in salt caverns and horizontal cavern construction technology. *Journal of Energy Storage*, *60*, 106489.

Prisecaru, P. (2022). The War in Ukraine and the Overhaul of EU Energy Security. *Global Economic Observer*, *10*(1).

Rahman, M. M., Oni, A. O., Gemechu, E., & Kumar, A. (2020). Assessment of energy storage technologies: A review. *Energy Conversion and Management*, *223*, 113295.

Schwab, L., Popp, D., Nowack, G., Bombach, P., Vogt, C., & Richnow, H. H. (2022). Structural analysis of microbiomes from salt caverns used for underground gas storage. *International Journal of Hydrogen Energy*, *47*(47), 20684–20694. https://doi.org/10.1016/j.ijhydene.2022.04.170

Steward, D., Saur, G., Penev, M., & Ramsden, T. (2009). *Lifecycle cost analysis of hydrogen versus other technologies for electrical energy storage* (tech. rep.). National Renewable Energy Lab.(NREL), Golden, CO (United States).

Thiyagarajan, S. R., Emadi, H., Hussain, A., Patange, P., & Watson, M. (2022). A comprehensive review of the mechanisms and efficiency of underground hydrogen storage. *Journal of Energy Storage*, *51*, 104490. https://doi.org/10.1016/j.est.2022.104490

TNO. (n.d.). *Informatiebladen: Zoutwinning*.

UNFCCC, V. (2015). Adoption of the Paris Agreement. I: proposal by the president (Draft Decision). *United Nations Office, Geneva (Switzerland)*, 32.

van Gessel, S. F., Huijskes, T., Juez-Larre, J., & Dalman, R. (2021). Ondergrondse Energie opslag in Nederland 2030-2050: ontwikkelpaden en aanbevelingen.

Wijermans, E. A. M. (2013). Geomechanical modelling and subsidence prediction of salt deposits for solution mining.

Williams, J. D., Williamson, J., Parkes, D., Evans, D. J., Kirk, K. L., Sunny, N., Hough, E., Vosper, H., & Akhurst, M. C. (2022). Does the United Kingdom have sufficient geological storage capacity to support a hydrogen economy? Estimating the salt cavern storage potential of bedded halite formations. *Journal of Energy Storage*, *53*, 105109. https://doi.org/10.1016/j.est.2022.105109

Yousefi, S. H., Groenenberg, R., Koornneef, J., Juez-Larré, J., & Shahi, M. (2023). Techno-economic analysis of developing an underground hy-

drogen storage facility in depleted gas field: A dutch case study. *International Journal of Hydrogen Energy*.

Zhang, X., Liu, W., Jiang, D., Qiao, W., Liu, E., Zhang, N., & Fan, J. (2021). Investigation on the influences of interlayer contents on stability and usability of energy storage caverns in bedded rock salt. *Energy*, *231*, 120968.

Zhu, S., Shi, X., Yang, C., Li, Y., Li, H., Yang, K., Wei, X., Bai, W., & Liu, X. (2023). Hydrogen loss of salt cavern hydrogen storage. *Renewable Energy*, *218*, 119267.

Appendix

Table A1. *All parameters used in the model which have not been mentioned in the text, in order of use in the model.*

Parameter	**Symbol**	**Value**
Temperature in the cavern (K)	T_{cavern}	300
Overburden pressure (Pa/m)		22620.6
Density of hydrogen (kg/m^3)	ρ_{H_2}	0.08375
Lower heating value of hydrogen (kWh/kg)	LHV_{H_2}	33.33
Ideal gas constant ($J/mol * K$)	R	8.314
Molar mass of hydrogen (g/mol)	MM_{H_2}	2